ISTITUTO NAZIONALE DI FISICA NUCLEARE

Sezione di Milano

INFN/TC-03/14
7 Ottobre 2003

THE STUDY OF THE NOISE OF SILICON JFET TRANSISTORS IN A WIDE TEMPERATURE RANGE

C. Arnaboldi[1], A. Fascilla[1], Mark W. Lund[2], G. Pessina[1]

[1)] INFN, Istituto Nazionale di Fisica Nucleare and Università degli Studi di Milano-Bicocca, P.za della Scienza 3, 20126 Milano IT
[2)] Lund Instrument Engineering, Inc., 140 South Mountainway Drive, Orem UT 84058, USA

Abstract

Different low noise JFET processes that have shown outstanding dynamic and noise performance at both room temperature and low temperatures have been selected. For most of them we have been able to detect the presence of shallow individual traps at low temperature, which create low frequency Generation-Recombination (G-R) noise. For one device type no evidence of traps has been observed at the optimum temperature of operation (around 100□K). It had a very small residual low frequency noise. This device has been cooled down to 14 K. From below 100 K down to 14□K the noise was observed to increase due to G-R noise originating from donor atoms (dopants) inside the channel. A very simple theoretical interpretation confirms the nature of G-R noise from these very shallow trapping centers. We also studied devices from a process optimized for room temperature operation and found noise corresponding to the presence of a single deep level trap. Even for this circumstance the theory was experimentally confirmed. The measurement approach used allowed us to achieve a very high accuracy in the modeling of the measured G-R noise. The ratio of the density of the atoms responsible for G-R noise above the doping concentration, N_T/N_d, has been verified with a sensitivity around 10^{-7}.

PACS: 07.50.-e, 07.50.Ek, 07.50.Yd, 84.30.-r, 84.30.Le, 84.30.Yq, 85.30.De, 85.30.Tv, 85.40.Qx.

Published by ***SIS–Pubblicazioni***
Laboratori Nazionali di Frascati

1 INTRODUCTION

There is a large demand for devices to be operated at low temperature, having both small series noise at small frequency and low parallel noise. One class of applications, from which this work was started, is bolometers[1)], which are large impedance detectors[2)] that generate slow signals and are able to reach very high energy resolution[3)].

A systematic study and selection of transistor properties has been made for the readout of bolometric detectors for two requirements: the first stage (located at cryogenic temperature) and the second stage (located at room temperature). Silicon JFETs have been investigated for both cases since they have superior low frequency and parallel noise performances.

The study and interpretation of G-R noise is also important for applications where the devices operate in the presence of radiation[4), 5)] such as space applications or experiments that make use of particle accelerators.

In this paper we present the results obtained in the selection of transistor processes optimized for cryogenic operation and transistor processes optimized for room temperature operation. Accurate investigation has been made with regards to the low frequency (LF) region of the noise spectra. Since the transistors selected showed very outstanding performances, a very accurate investigation was possible that confirmed the Generation-Recombination, G-R, nature of noise coming from individual traps. At very low temperatures the noise limit of silicon JFETs was proven to be due to G-R noise coming from the dopant atoms acting as traps. An analysis was developed for interpreting the measured data.

Two different set-ups were used for temperature characterization. JFETs optimized for room temperature operation were measured inside an environmental chamber. The temperature was varied from -60 ^{O}C to +70 ^{O}C.

To implement a setup for systematic transistor characterization at cryogenic temperatures, we have developed a special apparatus that is able to cool the transistors without the need of any pumping system. This was found necessary for precise characterization of the low frequency region of the noise spectra measured. The noise of the Device transistor Under Test (DUT) was readout by an amplifier with well-characterized low noise performance, that was possible to subtract from the overall noise measured. The collected data has been analyzed with fitting algorithm based on the χ-square technique.

In the following section the analysis of the expected noise behavior is performed. Then the development of the cryogenic system and second amplifier stage will be addressed, including the selection of an input transistor with a negligible Generation-Recombination (G-R) noise at low frequencies. In sections 4 to 7 the experimental results of the low temperature noise measurement of the selected transistors will be shown in detail.

Since the many symbols and parameters used in the text, we included Table 1 that is a reference/summary of all the mathematical definitions used. The reader should refer to this Table whenever parameters are not defined in the text.

Table 1: List of symbol used in the paper.

LIST OF SYMBOLS USED IN THE TEST	
a metallurgical channel thickness.	N_d concentration of donor atoms, $1/cm^3$.
A_{LOR} noise amplitude coefficient of the G-R noise generated by a trap.	N_T concentration of the trapping centers, $1/cm^3$.
C_G input capacitance of a totally depleted JFET, $=\varepsilon a/LZ$.	N_{Tv} electron present in the conduction band in the volume V, $N_{Tv}=N_T V$.
c_n, c_p capture probability per unit time of an electron (hole) from a trapping center, $c_{n(p)}=\sigma_{n(p)} v_{th[el(ho)}$.	N_V number of available states in the valence band, $\approx 2\left[2\pi\pi_B T m_h / h^2\right]^{3/2}$.
e electron charge, 1.6×10^{-19} C.	N_{Vv} number of available states in the valence band in the volume V, $N_{Vv}=N_V V$.
e_n, e_p emission probability per unit time of an electron (hole) from a trapping center.	p instantaneous concentration of free holes in the valence band, $1/cm^3$.
E_C Energy of the conduction band (eV).	p_{po} holes concentration in the valence band in thermal equilibrium in the p region.
E_d Energy of the donor center within the energy gap (eV).	p_1 holes concentration obtained if the Fermi level is at the trap energy E_T, $p_1 = [(N_T - n_{To})/n_{To}]p_o = = N_V \exp\left(\frac{E_V - E_T}{K_B T}\right)$
E_F Quasi-Fermi Energy.	
E_T Energy of the trapping centers within the energy gap (eV).	
f_{LOR} −3 dB frequency for the Lorentzian trap.	
f_d Fermi factor for donors ($=1/(1+\exp(E_d-E_{Fd})/K_B T$, E_{Fd}=quasi Fermi level for donors).	p_o stationary concentration of free holes in the valence band, $= N_V \exp((E_V - E_F)/K_B T)$.
f_T Fermi factor for traps at energy E_T ($=1/(1+\exp(E_T-E_{FT})/K_B T$, E_{FT}=quasi Fermi level for traps).	R_{ce} rate of capture of electrons from the trapping centers, $R_{ce}=c_n(N_T-n_T)n$.
G-R Generation and Recombination.	R_{ee} rate of emission of electrons from the trapping centers, $R_{ee}=e_n n_T$.
g_d degeneration factor for electrons on donor sites, g_d=integer, ≥ 1.	R_{ch} rate of capture of holes from the trapping centers, $R_{ce}=c_p(N_T-n_T)p$.
g_T degeneration factor for electrons on trapping centers sites, g_T=integer, ≥ 1.	R_{eh} rate of emission of holes from the trapping centers, $R_{eh}=e_p n_T$.
h Planck constant, 6.626×10^{-34} Js.	T absolute temperature.
K_B Boltzmann constant, 1.38×10^{-23} J/K.	τ typical trap time constant, $=1/2\pi f_{LOR}$.
I_{DS} drain to source current of a JFET.	$v_{th[el(ho)}$ thermal velocity of electron (hole), $V_{th[el(ho)]} = \sqrt{3K_B T / m_{n(h)}}$
I_{DSS} maximum drain to source current, obtained at V_{GS}=0 V, of a JFET.	V_{bi} built-in potential for a pn junction, $V_{bi} = (K_B T/q)\ln\left(n_{no} p_{po} / n_i^2\right)$.
L gate length.	
LF Low Frequency.	
m_n electron reduced mass (Kg).	$\overline{v_{gndr}^2}$ gate noise due to G-R centers present in the depletion region.
m_e electron mass (Kg).	
m_h hole mass (Kg).	
n instantaneous concentration of free	

electrons in the conduction band, $1/cm^3$.

n_o stationary concentration of free electrons in the conduction band, $= N_C \exp((E_F - E_C)/K_B T)$.

n_{no} electron concentration in the conduction band in thermal equilibrium in the n region.

n_{ov} electron present in the conduction band in the volume V, $n_{ov}=n_o V$.

n_d electrons trapped at donor centers, $n_d \approx N_d$ at room temperature.

n_{dv} electrons present in the conduction band in the volume V, $n_{dv}=n_d V$.

n_T instantaneous concentration of the electrons trapped at energy E_T, $1/cm^3$.

n_{To} stationary concentration of the electrons trapped at energy E_T.

n_{Tov} electrons trapped at E_T in the volume V, $n_{Tov}=n_{To} V$.

n_1 electron concentration obtained if the Fermi level were at the trap energy E_T, $n_1 = [(N_T - n_{To})/n_{To}]n_o = == N_C \exp\left(\frac{E_T - E_C}{K_B T}\right)$.

N_a acceptor type concentration.

N_C number of available states in the conduction band, $\approx 2\left[2\pi K_B T m_n / h^2\right]^{3/2}$.

N_{Cv} number of available states in the conduction band in the volume V, $N_{Cv}=N_C V$.

$\overline{v_{nch}^2}$ gate noise due to G-R centers present in the channel region.

V_G voltage at the gate terminal of a JFET.

V_S voltage at the source terminal of a JFET.

V_D voltage at the drain terminal of a JFET.

V_P pinch-off voltage, $V_P = q n_{no} a^2 / 2\varepsilon$.

V_T threshold voltage, $V_T=V_{bi}-V_P$.

Z gate width.

W gate thickness, position and bias dependent inside the channel.

ε dielectric permittivity of silicon, $\varepsilon_r\varepsilon_o=105.4$ pF/m.

μ charge mobility.

σ capture cross section, cm^2.

ν_e rate of emission of a charge carrier from a trapping center, $\nu_e=1/\tau_e$.

ν_c rate of capture of a charge carrier from a trapping center, $\nu_c=1/\tau_c$.

2 THE ANALYSIS OF LOW FREQUENCY NOISE COMING FROM DEEP AND SHALLOW TRAPS

Low frequency (LF) noise coming from the trapping mechanism has been extensively studied. In this paper we will give an overview of the analysis of deep trapping center behavior and detail the theory for the factors affecting the shallow level centers, specifically the donor sites, at very low temperature. We have selected very low noise silicon JFET transistors to prove the theories experimentally. A very high accuracy has been reached thanks to the very low noise levels measured, around and below 1 nV/√Hz at both room temperature and low temperature, obtaining high sensitivity in the temperature dependence of the trapping centers. Although at very low temperature LF noise from dopant sites has a large

frequency corner, we will show that it is possible to detect it and we will prove its effects on the noise performance.

It has to be considered that other mechanisms may generate LF noise[6] that are not found to operate in the transistors we have selected. In addition, the G-R noise manifests itself with different frequency behaviors (typically f^{-1} slope), in some devices (typically MOS transistors). In those cases electrons can tunnel into the oxide that is located above the channel, remaining trapped for a time that depends on how deep the tunnelling path was[7, 8]. Extensive study has been done on the mechanism responsible of LF noise in MOS transistors[9, 10, 11].

Let us now discuss the origination of G-R noise. Let us suppose to be present inside a semiconductor slab, in which a current can flow, a concentration of at least one specie of atoms with energy levels within the band gap that are able to capture or emit electrons or holes. Each time a charge carrier is captured (or recombined) for an interval of time t_T the current is diminished by one unit. The reverse is true when a charge carrier is emitted (or generated). If the process is randomly distributed a noise is thus created with a spectrum which is correlated to the typical time interval t_T of this trapping or de-trapping process. If more recombination center sites exist having different time constants, t_T, the shape of the noise spectrum will result as the superposition of each process.

The behavior of the G-R process is interpreted with the principle of the 'detailed balance'[12, 13, 14], which states that at thermal equilibrium the net rate of capture of electrons (holes) must balance the net rate of generation of electrons (holes). After any external perturbation of this situation, the system relaxes again to the equilibrium condition. This happens with a time dependence that is related to the kind of G-R centers that are involved in the process.

We are interested in how noise is generated from the stationary condition. Charge carriers can make transitions from/to the trapping centers after having been absorbed/released at random energy from/to the lattice, at temperature T, as described above. Although the detailed balance is maintained on the average since T is stationary, if a current is flowing into the device, instantaneous changes of its value will happen as a consequence of the random process of trapping/de-trapping of charges from the centers, filled around the stationary state, generating noise signals. In some situations the effect of the processes can be seen as a sequence of square pulses known as 'Random Telegraph Signals', RTS[15, 16, 17]. The RTS are the manifestation in the time domain of the G-R noise. As said above a trapping/de-trapping of a single charge results in current pulse. Let us try to quantify it. In an n-region of a semiconductor where a current is flowing we can write:

$$I = enA\mu \frac{V_{BIAS}}{L} = eN_{TOT}\mu \frac{V_{BIAS}}{L^2} \tag{1}$$

where A is the cross section, L the sample length and V_{BIAS} the applied bias voltage. If a charge is freed from a trap the total number of charges N_{TOT} will increase: $N_{TOT} \rightarrow N_{TOT}+1$.

Consequently[18)]

$$\Delta I = \frac{I}{N_{TOT}} = \frac{I}{nAL}; \tag{2}$$

the current change due to a single charge is measurable if it is larger than the peak-to-peak noise. From the above equation this is verified when the charge concentration and/or the device are very small. An example of the above interpretation is shown in Figure 1. There the parallel noise of a small Heterojunction Bipolar Transistor at 4.2 K temperature is developed across 100 kΩ resistor and is amplified a factor of 10000 V/V. A few nA pulses are clearly visible above the noise floor.

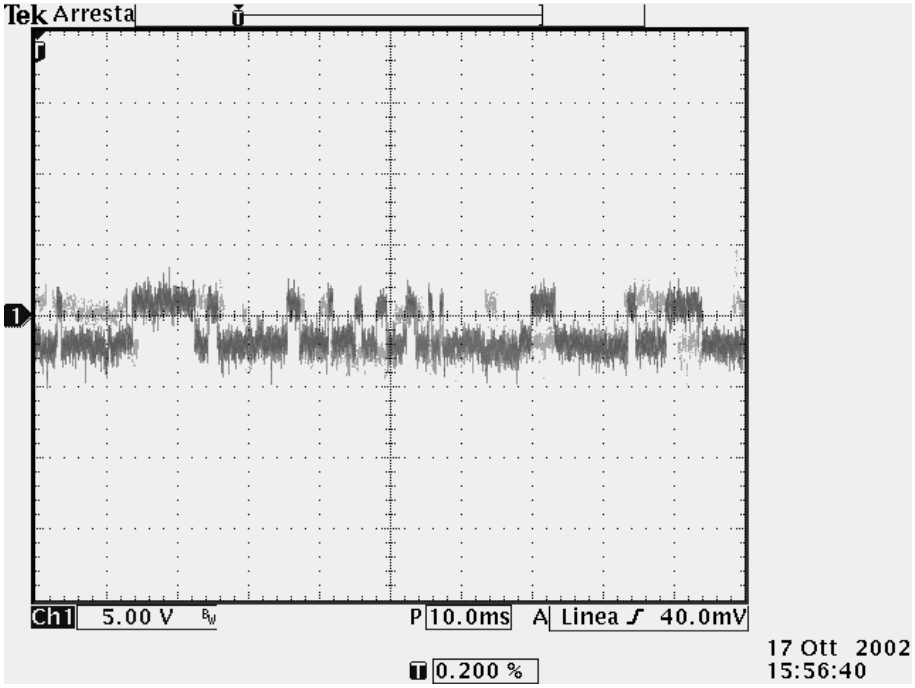

Figure 1: RTS noise developed across 100 KΩ resistor by the parallel noise of a SiGe Heterojunction Bipolar transistor at 4.2 K temperature. The noise has been amplified 10000 V/V.

The mathematical description of the G-R noise mechanism is simple when a single kind of G-R center dominates the process. When different types of G-R centers are present the overall effect can be calculated by the superimposition of the noise contribution of each center, once a certain degree of correlation is taken into account. The interpretation of the measurement is more complicated in this case, although for two or three trapping centers some evaluation can be made[19), 20), 21)].

The mathematical model for the G-R noise is known[22), 23), 24), 25)]. In this paper we will address the results in a simple form. At the same time emphasis will be on the G-R noise effect coming from the shallow donor centers at cryogenic temperatures.

2.1 General Theory of Generation Recombination Noise

Let's suppose that a single type of G-R center having a concentration N_T ($1/cm^3$) dominates the noise with an activation energy of E_T eV above the valence band, taken as the reference level. The rate of change of the concentration n_T of electrons present at the trapping centers after a small, arbitrary, excitation h(t) is given will satisfy the equation:

$$\frac{dn_T}{dt} = (R_{ce} - R_{ee}) - (R_{ch} - R_{eh}) - h(t) \tag{3}$$

where R_{ce} and R_{ch} are the capture rate for the electrons and holes respectively, while R_{ee} and R_{eh} are the emission rate for electrons and holes. R_{ce} is given by the product of the probability per unit time and unit volume that an electron is captured, c_n, the number of free trapping centers, N_T-n_T, and the number of electrons in the conduction band, n, $R_{ce}=c_n(N_T-n_T)n$. With a similar consideration $R_{ch}=c_p n_T p$. R_{ee} is instead given by the product of the probability per unit time that an electron is emitted from a trap, e_n, and the number of electrons trapped, n_T, $R_{ee}=e_n n_T$. With a similar consideration $R_{eh}=e_p(N_T- n_T)$. Equation (3) can then be rewritten:

$$\frac{dn_T}{dt} = (c_n n + e_p)N_T - (c_n n + c_p p + e_n + e_p)n_T - h(t) \tag{4}$$

From eq.(4) a number of facts can be extracted. The perturbation h(t) is supposed to exist for a short interval of time, so we expect that at large time n_T equals the initial, equilibrium, value, hence: $(dn_T/dt)|_\infty = 0$. At large times eq.(4) reduces to:

$$\left.\frac{dn_T}{dt}\right|_\infty = 0 = [c_n n_o N_T - c_n n_o n_{To} - e_n n_{To}] + [e_p N_T - c_p p_o n_{To} - e_p n_{To}] \tag{5}$$

At thermal equilibrium the detailed balance applies and the emission of electrons must be equal to its inverse process, capture of electrons. The same consideration applies to holes[14]. This implies that both terms inside the squared parenthesis must be equal to zero. From this we can get the relation between e_n and c_n, e_p and c_p:

$$e_n = c_n \frac{N_T - n_{To}}{n_{To}} n_o = c_n n_1 \qquad e_p = c_p \frac{n_{To}}{N_T - n_{To}} p_o = c_p p_1 \tag{6}$$

After any perturbation, an unbalance in the recombination rate will result that will try to restore the original situation. From eq.(6) we can rewrite eq.(4):

$$\frac{dn_T}{dt} = [c_n n + c_p p_1]N_T - [c_n(n + n_1) + c_p(p + p_1)]n_T - h(t) \tag{7}$$

In this differential equation the functions n, p and n_T are not necessary independent. The cases of interest are considered in the following.

2.1.1 G-R noise in a depletion region of a pn junction

The first interesting case is when eq.(7) is applied to the depletion region of a pn junction. In this situation the concentration n and p reduce to negligible values. Any instant a

charge is generated from a trapping center, it is swept away in a very short time, equal to the transit time across the junction. Since the depletion region is almost depleted from free carriers, only generation processes are possible, as shown in Figure 2: electrons emitted from trapping centers into the conduction band and holes emitted in the valence band, that is electrons captured from the valence band.

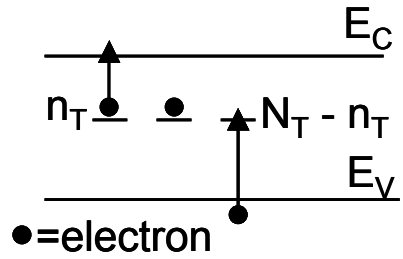

Figure 2: The more probable electron and hole emission processes from a deep trapping center in the depletion region of a reverse biased pn junction. Black circles represent electrons.

The resulting population n_T is therefore independent from n_o and p_o and eq.(7) can be written:

$$\frac{dn_T}{dt} = \left[c_n n_o + c_p p_1\right] N_T - \left[c_n (n_o + n_1) + c_p (p_o + p_1)\right] n_T - h(t) \tag{8}$$

The concentrations n_o and p_o strongly depend on the applied voltage in the reverse region, the concentrations being negligible in the deep part of its extension. If we assume that the excitation h(t) is very short in comparison to the response time of the system we can approximate $h(t)=h_A\delta(t)$, $h_A>0$, and represent eq.(8) in the following way:

$$\tau \frac{dn_T}{dt} = \left[c_n n_o + c_p p_1\right] \tau N_T - n_T - \tau h_A \delta(t), \qquad \tau = \frac{1}{c_n (n_o + n_1) + c_p (p_o + p_1)}. \tag{9}$$

In the expression above for n_T the first term represents the stationary condition. The solution of the differential equation is:

$$n_T(t) = \left[c_n n_o + c_p p_1\right] \tau N_T - h_A \exp(-t/\tau) 1(t), \qquad 1(t) = \begin{cases} 1 & t > 0 \\ 0 & t \le 0 \end{cases}, \quad \frac{d1(t)}{dt} = \delta(t). \tag{10}$$

There is the superimposition of two effects that determines the time constant τ: capture and emission of charge carriers. We expect that τ is dominated by the slower of the two processes. If eq.(3) is rewritten by supposing only the emission of electrons in both the conduction and valence bands, namely $R_{ce}=R_{eh}=0$, it is possible to come to an expression similar to eq.(9) but with a time constant, τ_e, given by:

$$\tau_e = \frac{1}{c_n n_1 + c_p p_o}. \tag{11}$$

An analogous consideration leads to the capture time constant τ_c of electrons from the valence and conduction bands, once the approximation $R_{ee}=R_{ch}=0$ is made:

$$\tau_c = \frac{1}{c_n n_o + c_p p_1}. \tag{12}$$

The combination of the two effects leads to a time constant, τ, given by:

$$\frac{1}{\tau} = \frac{1}{\tau_e} + \frac{1}{\tau_c}; \tag{13}$$

which coincides with what has been obtained in eq.(9).

The equilibrium condition for n_T should be given by the product of N_T times the probability of having a charge trapped at the energy E_T. If ν_e ($\nu_e=1/\tau_e$) and ν_c ($\nu_c=1/\tau_c$) are the emission and capture rates, respectively, the probability of finding a charge at the trap level is given by:

$$p_c = \frac{\nu_c}{\nu_c + \nu_e} \qquad \text{or} \qquad p_c = \frac{\tau_e}{\tau_c + \tau_e}; \tag{14}$$

so we expect that:

$$n_T(\infty) = \frac{\tau_e}{\tau_c + \tau_e} N_T, \tag{15}$$

which is what it is given in the first term of eq.(9).

In evaluating eq. (10) no assumptions have been made in considering whether the trapping center is an acceptor or a donor. This means that it is impossible to determine the nature of the process responsible for the noise from a noise measurement.

To implement a model useful for the noise evaluation we consider the response to a small perturbation away from the equilibrium condition. From eq.(10) this is given by the quantity $\Delta n_T(t)$ given by:

$$\Delta n_T(t) = n_T(t) - n_T(\infty), \tag{16}$$

or:

$$\Delta n_T(t) = -h_A \exp(-t/\tau) 1(t). \tag{17}$$

Noise is better studied in the frequency domain, so we consider the Fourier transform of the above relation:

$$\Delta n_T(\omega) = -\frac{\tau}{1 + j\omega\tau} h_A. \tag{18}$$

We can now identify the generic excitation $h_A\delta(t)$ with a noise source. The variable $\Delta n_T(\omega)$ is the response of a linear system. If we input a noise source having a spectrum $\overline{h_n^2}(\omega)$ to a linear system we get an output given by the product of the square of the modulus of the

system response to a δ(t)-like excitation and the input noise. From eq.(18) we can therefore write:

$$\overline{\Delta n_T^2(\omega)} = \frac{\tau^2}{1+(\omega\tau)^2}\overline{h_n^2(\omega)}\,. \tag{19}$$

In this case the noise source is the random, temperature dependent generation/recombination of charge carriers. This random process is independent of frequency and produces a white spectrum, $\overline{h_n^2(\omega)} = \overline{h_N^2}$. The statistics that lead to its evaluation are described in subsection 2.2.

Eq. (19) shows that the response to a white noise source of a G-R process has a Lorentzian shape.

2.1.2 G-R noise in a doped region

In an n-doped region, or also in a forward biased junction away from the transition region, there is a correlation between the free electrons in the n region and the trapped or emitted carriers. Since a large number of carriers are present in the conduction band, the trapping levels are active with the process indicated in Figure 3: capture/emission from/to the conduction band. A similar argument is valid for the holes in the p region.

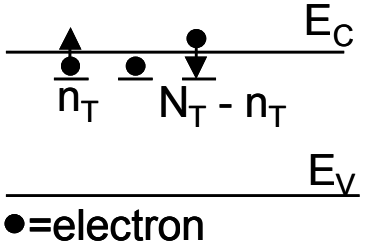

Figure 3: Emission and capture processes from a shallow trapping center in a forward biased pn junction. Black circles represent electrons.

When a single type of acceptor trap is dominant we have $n=N_d-n_d-n_T\approx N_d-n_T$. Equation (7) becomes:

$$\frac{dn}{dt} = c_n n_1 N_d - c_n\left(N_T - N_d + n_1\right)n - c_n n^2 + h_A\delta(t)\,. \tag{20}$$

If the traps are donors $n\approx N_d+(N_T-n_T)$. An equation similar to eq. (20) is obtained by substituting N_d+N_T for N_d . Finally, if we consider the dopant atoms as donor traps themselves then $n\approx N_d-n_d$ and again an equation similar to eq.(20) is obtained by making the substitution $N_T=N_d$.

So, regardless of the kind of traps, the differential equation that is obtained is of the form:

$$\frac{dn}{dt} = A - Bn - C n^2 + h_A \delta(t) . \qquad (21)$$

For the three cases considered above the coefficients A, B, and C are given in Table 2.

Table 2: Coefficients for the differential eq.(21) for the 3 cases: acceptors, donors and n-donor doping centers.

Trap type	A	B	C
Acceptor centers	$c_n n_1 N_d$	$c_n(N_T-N_d+n_1)$	c_n
Donor centers	$c_n n_1(N_T+N_d)$	$c_n(n_1-N_d)$	c_n
Dopants	$c_n n_1 N_d$	$c_n n_1$	c_n

The differential equation above has been solved in the past using two approximations: operation at room temperature[22] or at very low temperature[26]. To extend the analysis over a wide temperature range we derived in Appendix A the solution of eq.(21) for any condition. The result is:

$$n(t) = \frac{-B+\sqrt{B^2+4AC}}{2C} + \frac{1(t)}{\left[\frac{C}{\sqrt{B^2+4AC}} + \frac{1}{h_A}\right] \exp\left(\left(\sqrt{B^2+4AC}\right)t\right) - \frac{C}{\sqrt{B^2+4AC}}} . \qquad (22)$$

We are interested in small perturbations of the equilibrium condition. The equation above can therefore be approximated to:

$$n(t) \approx \frac{-B+\sqrt{B^2+4AC}}{2C} + h_A \exp\left(-\left(\sqrt{B^2+4AC}\right)t\right) 1(t) . \qquad (23)$$

The equilibrium condition and the recovery time constant of eq.(23), $\tau = 1/\sqrt{B^2+4AC}$, are given in Table 3 for different kinds of traps. We can see that for deep acceptors and donors, the time constants are very small compared with those given in the depletion region. At very low temperatures dopant trap recovery is governed by a time constant that increases as the temperature decreases.

In analogy with the considerations that led to eq.(19) of the previous subsection, applied now to the approximated linear response given in eq.(23), we can calculate $\Delta n(t)=n(t)-n(\infty)$ in the frequency domain as:

$$\Delta n(\omega) = -\frac{\tau_c}{1+j\omega\tau_c} h_A \qquad \tau_c = \frac{1}{\sqrt{B^2+4AC}} . \qquad (24)$$

Thus the noise will be:

$$\overline{\Delta n^2(\omega)} = \frac{\tau_c^2}{1+(\omega\tau_c)^2}\overline{h_n^2(\omega)}. \tag{25}$$

The noise shape is similar to the one obtained in eq.(19), except that the time constant is different.

Table 3: Stationary condition and recovery time constant for eq.(23) for different trapping types in a forward biased pn junction.

Trap type	$\tau = \frac{1}{\sqrt{B^2+4AC}}$	**n(∞)**
Acceptor centers	$\approx \frac{1}{c_n(N_d+N_T+n_1)}$	N_d-N_T
Donor centers	$\approx \frac{1}{c_n(N_d+2N_T+n_1)}$	N_d
Donor dopants	$\frac{1}{c_n(2n_o+n_1)}$	T=300 K: N_d-n_{do}
	T→0 K: $\approx \frac{1}{c_n n_o}$	T→0 K: n_o

2.2 Counting statistics

Equation (19) and eq. (25), that has similar shape, give the fluctuation that we expect in the charge carrier population as a response to a random perturbation $\overline{h_n^2(\omega)}$. Now we try to quantify $\overline{h_n^2(\omega)}$.

The integration of the fluctuating quantities over the whole frequency range results in the overall Root Mean Square, RMS, fluctuation Δn_{RMS}^2, once it is considered that $\overline{h_n^2(\omega)} = \overline{h_N^2}$, chosen monolateral:

$$\Delta n_{RMS}^2 = \frac{1}{2\pi}\int_0^\infty \frac{\tau}{1+(\omega\tau)^2}\overline{h_A^2(\omega)}df = \frac{1}{4}\tau\overline{h_N^2}, \tag{26}$$

so:

$$\overline{h_N^2} = \frac{4\Delta n_{RMS}^2}{\tau}, \tag{27}$$

and thus:

$$\overline{\Delta n^2(\omega)} = 4\frac{\tau}{1+(\omega\tau)^2}\Delta n^2_{RMS}. \tag{28}$$

Δn^2_{RMSv} has so far been evaluated following different approaches and approximation. For the statistical mathematical evaluation, we need to consider dimensionless quantities. We therefore consider the fluctuation of the total number of carriers contained within a volume V, $n_{Tv}=n_T V$, $N_{Tv}=N_T V$, etc. V may of course depend on position within the semiconductor.

The simpler approach in determining Δn^2_{RMSv} is to consider the G-R process governed by a binomial distribution that allows expressing $\Delta n^2_{RMSv} = (1-p)\,pN_{Tv}$, p being the probability to find a charge trapped at the energy ET, equal to eq.(14) [20]. A more accurate approach is based on thermodynamics[27), 28), 29)]. Further, a statistical method based on an inductive evaluation has also been used[30)]. Finally, a classical statistical approach has been given based on the Stirling formula[31)] and Lagrange multipliers, from which the classical Fermi distribution functions are obtained. We refer to this last approach for the determination of the fluctuation of the number of free carriers, since this way it is proven that G-R noise is generated by a fluctuation of the stationary state of the electron system. We will summarize it very briefly, referring to refs.[19)] and[31)] for further details.

As it is well known, the Fermi distribution function describes the charge distribution of a system with many levels of energies E_i having each N_{iv} available states, n_{iv} of which are filled, and N_{iv}-n_{iv} are unfilled. Let n_{totv} denote the total number of charges present, electrons or holes. The Fermi distribution is obtained by finding the probability distribution of the charges among these levels, subject to the constraints that the total number of charges and available energy remains constant. The application of the Stirling approximation to the permutations within each level, and then the application of the Lagrange multipliers to the resulting distribution allow maximizing the probability of the system. It can be proved[31)] that the distribution of any of the variables $\Delta n_{iv}=n_{iv}-n_{iov}$ is normal at least around its stationary condition, as can be expected. The probability $p(\Delta n_{iv1}, \Delta n_{iv2},\cdots)$ of having the given combination $\Delta n_{iv1}, \Delta n_{iv2},\cdots$ results:

$$p(\Delta n_{iv1}, \Delta n_{iv2},\cdots) \div \exp\left(-\frac{\Delta n^2_{iv1}}{2\sigma_1^2}\right)\exp\left(-\frac{\Delta n^2_{iv2}}{2\sigma_2^2}\right)\cdots. \tag{29}$$

where σ_i is the RMS fluctuation expected from a single variable, given by the binomial distribution:

$$\sigma_i^2 = p_i(1-p_i)N_{iv} = \left(\frac{1}{n_{iv}}+\frac{1}{N_{iv}-n_{iv}}\right)^{-1}. \tag{30}$$

If many levels are present the probability of finding a given Δn_{iv}, $P(\Delta n_{iv})$, irrespective of any other occupation combination, but with the constraint of the constant value of the total

number of charges present, after integration above any Δn_{kv}, with $k \neq i$, can be shown to be approximated by:

$$P(\Delta n_{iv}) \div \exp\left(-\frac{\Delta n_{iv}^2}{2\sigma_i^2}\right). \tag{31}$$

Let us now consider a two level system composed of the conduction band, with N_{cv} states available, and a trap level, with N_{Tv} states available. The expression n_{totv} is the total number of electrons that can occupy the available states, $n_{totv} << N_{cv}$. By definition, n_v electrons from n_{totv} will be at N_{cv}, and n_{Tv} at N_{Tv}, such that:

$$\begin{cases} N_{cv} + N_{Tv} - n_{totv} = (N_{cv} - n_v) + (N_{Tv} - n_{Tv}) \\ n_v E_{cv} + n_{Tv} E_{Tv} = \text{Cost.} \\ n_{totv} = n_v + n_{Tv} \end{cases}. \tag{32}$$

The application of the considerations made above to such a simple situation, allows reducing eq. (29) to:

$$p(\Delta n_V, \Delta n_{Tv}) \div \exp\left(-\frac{\Delta n_v^2}{2\sigma_n^2}\right) \exp\left(-\frac{\Delta n_{Tv}^2}{2\sigma_{n_T}^2}\right). \tag{33}$$

From eq. (32) $\Delta n_v = -\Delta n_{Tv}$, so for the simple case of a two level system $P(\Delta n_v)$ results:

$$P(\Delta n_v) = \exp\left(-\frac{1}{2}\left(\frac{1}{\sigma_n^2} + \frac{1}{\sigma_{n_T}^2}\right)\Delta n_v^2\right) \tag{34}$$

Or:

$$\begin{aligned} \frac{1}{\Delta n_{RMSv}^2} &= \frac{1}{\sigma_n^2} + \frac{1}{\sigma_{n_T}^2} = \frac{1}{n_{ov}} + \frac{1}{N_{cv} - n_{ov}} + \frac{1}{n_{Tov}} + \frac{1}{N_{Tv} - n_{Tov}} \\ &\approx \frac{1}{n_{ov}} + \frac{1}{n_{Tov}} + \frac{1}{N_{Tv} - n_{Tov}} \end{aligned}. \tag{35}$$

The term that contains N_{cv} has been neglected in the last result since the concentration used to dope JFET channels is always much smaller than the concentration of the available states in the conduction band.

The boundary condition given in eq. (32) imposes a correlation between the number of electrons present in the conduction band and the number present at the trap levels. The degree of correlation is negligible when n is much greater than the trapping center concentration. This is not the case at low temperatures when the trapping centers are the dopant atoms themself.

When we consider a reverse junction, any charge created in the conduction band is swept away in a very short time, n_v is therefore negligible, does not fluctuate and can be neglected in eq.(32). As a result Δn^2_{RMSv} is contributed only by the variance of n_{Tv}. In an n-region, or in a forward biased pn junction away from the transition region, the variance is dependent only on the trapping center concentration N_T any time this concentration is much smaller than the doping concentration, $N_T << N_d, N_c$, which is the typical situation, opposed to the one just described.
For both these cases we therefore have the same mathematical representation:

$$\Delta n^2_{RMSv} = \frac{n_{Tov}(N_{Tv} - n_{Tov})}{N_{Tv}}. \tag{36}$$

The last case we consider is the one in which the noise comes from the dopants themselves acting as traps. For this case we put $N_T=N_d$, and obtain:

$$\frac{1}{\Delta n^2_{RMSv}} = \frac{2}{n_{ov}} + \frac{1}{N_{dv} - n_{ov}} \quad \text{or} \quad \Delta n^2_{RMSv} = \frac{n_{ov}(N_{dv} - n_{ov})}{2N_{dv} - n_{ov}}. \tag{37}$$

The results above can be expressed in more detail if the probability of occupation of an energy level, f_T, the Fermi-Dirac distribution function, is introduced:

$$f_T = \frac{1}{1 + \exp[(E_T - E_F)/K_B T]} \tag{38}$$

E_F is the quasi-Fermi level, which depends on position, bias, and charge type within the semiconductor. Only one level for the quasi-Fermi level for every charge type is found at the equilibrium condition. From eq. (38) we find that the Fermi level, under equilibrium conditions, or the quasi-Fermi level, under non-equilibrium conditions, is the energy where the probability of electron occupancy is 1/2.

If g_T is the degeneracy factor for the electrons at the energy level E_T, we find that:

$$\frac{n_{To}}{N_T - n_{To}} = \frac{g_T f_T}{1 - f_T}. \tag{39}$$

Or:

$$n_{To} = f_T \frac{g_T}{1 + (g_T - 1) f_T} N_T \qquad N_T - n_{To} = (1 - f_T) \frac{1}{1 + (g_T - 1) f_T} N_T. \tag{40}$$

Finally, we have:

$$\begin{cases} \Delta n^2_{RMSv} = f_T(1-f_T)\dfrac{g_T}{[1+(g_T-1)f_T]^2}N_{Tv} & \text{Depleted region, or } n >> N_T \\ \Delta n^2_{RMSv} = f_d(1-f_d)\dfrac{g_d}{[1-f_d+2g_d f_d][1+(g_d-1)f_d]}N_{dv} & \text{Dopant trapping center effect.} \end{cases} . \quad (41)$$

In addition to the obtained results above it has to be considered that $\Delta n^2_{RMSv} = \Delta n^2_{RMS} V^2$.

From eq. (41) we can see that the noise is proportional to the product $f_T(1\text{-}f_T)$ which is a measure of how full a trapping level is. The equation's result says that a trapping level too full or too empty generates a negligible amount of noise. The maximum noise occurs when the trapping level is half full. At room temperature and higher, the capturing process competes with the emission process; both have a similar probability of occurring only for the deeper traps located close to the middle of the band gap. The shallow trapping centers, close to the conduction band energy, always have enough thermal energy to jump to the conduction band: they are therefore empty at all times and do not contribute to the G-R noise. As soon as the temperature lowers the shallow levels are more likely to be filled, while the deeper centers become filled most of the time. Consequently, the more effective centers for noise generation become the ones with energy closer to the conduction band.

An equivalent consideration can be made for the trapping center near the valence band.

A scan in temperature is therefore a useful way to study the presence and the effect of the trapping centers within the band gap.

2.3 G-R equivalent input noise in JFET

2.3.1 Gate noise due to G-R centers present in the depletion region

Let us now calculate the input-referred noise of a JFET due to the mechanisms described in the previous sub sections. We will start by calculating the noise generated in the depletion region of the JFET. Its effect can be regarded as a change in the gate voltage that arises from the fluctuation of the charge distribution present in the transition region. Given that only one kind of donor trap is present, the one-dimensional Poisson equation within the depletion region is:

$$\frac{dE}{dx} = \frac{e}{\varepsilon}[n_{no} + (N_T - n_T)] \quad \Rightarrow \quad E(x) = \frac{e}{\varepsilon}[n_{no} + (N_T - n_T)](x - W); \quad (42)$$

Here E(x) is the electric field and x has its origin at the gate, according to Figure 4.

The depletion region width is W and E(x) nulls at the edges of the depletion region. The positive concentration of ionized atoms is n_{no}, which is equal to N_d at ordinary temperatures. Let us consider the depletion region to be divided into sheets having thickness dx and volume

LZdx. The voltage drop across any sheet is: dv=-E(x)dx. This voltage may fluctuate at random due to fluctuations of n_T. Its variance $\delta v_{ndr}^2 = dv^2 - \overline{dv}^2$, according to (42), is ($\overline{\Delta n_T} = 0$):

$$\overline{\delta v_{ndr}^2} = \left(\frac{e}{\varepsilon}\right)^2 \overline{\Delta n_T^2}\,(x - W)^2 dx^2 ; \tag{43}$$

or:

$$\overline{\delta v_{ndr}^2} = \left(\frac{e}{\varepsilon}\right)^2 \frac{f_T(1-f_T)g_T}{[1+(g_T-1)f_T]^2}\frac{N_T}{LZdx}\frac{4\tau}{1+(\omega\tau)^2}(x - W)^2 dx^2 \ . \tag{44}$$

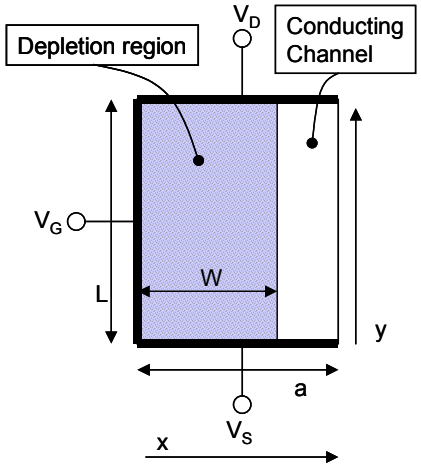

Figure 4: One dimensional model of a JFET in the saturation region. The width Z of the transistor is orthogonal to the paper.

The above equation must be integrated across the whole depletion region, (0,W). In principle both f_T and τ depend on position within (0,W). As a first approximation we can suppose τ and f_T to be constant within an interval ΔW_T around a position x_T, and zero outside. At the position x_T and within ΔW_T the total gate noise, $\overline{v_{gndr}^2} = \int_0^W \overline{\delta v_n^2}$ is:

$$\overline{v_{gndr}^2} = \left(\frac{e}{\varepsilon}\right)^2 \frac{f_{TW_T}\left(1-f_{TW_T}\right)g_T}{\left[1+(g_T-1)f_{TW_T}\right]^2}\frac{N_T}{LZ}\frac{4\tau_{W_T}}{1+\left(\omega\tau_{W_T}\right)^2}\Delta W_T(x_T - W)^2 . \tag{45}$$

In the above equation use has been made of eq. (41) and the depletion thickness has been approximated as constant across the channel. This last approximation is valid only in the saturation region. The terms f_{TW_T}, τ_{W_T} refer to the functions f_T and τ evaluated within ΔW_T. This approach has been used for the interpretation of the trap noise in MOS transistors due to shallow levels at low temperature[32), 33)]. In[33)] the parameters ΔW_T and x_T have been introduced to justify the interpretation of some discrepancies in interpreting the interpolated data in[34)] at temperature close to 100 K. If we make use of eq.(A.10) and eq.(A.13) of Appendix B, where

the main equations governing JFET operation in the saturation region are derived, we easily arrive to the expression:

$$\overline{v_{gndr}^2} = \frac{f_{TW_T}\left(1-f_{TW_T}\right)g_T}{\left[1+\left(g_T-1\right)f_T\right]^2}\,\frac{N_T}{n_{no}}\,\frac{8}{3}\,\frac{eV_P}{C_G}\,\frac{\tau_{W_T}}{1+\left(\omega\tau_{W_T}\right)^2}\left[\frac{3\Delta W_T\left(x_T-W\right)^2}{a^3}\right]; \tag{46}$$

where C_G is the input capacitance of the fully depleted JFET, $C_G=\varepsilon LZ/a$.

The equation above is proportional to the ratio of the trapping center concentration to the donor concentration and on some other measurable coefficients. The temperature dependence of this equation is quite complicated, depending on many parameters: f_{TW_T}, τ_{W_T} and ΔW_T and x_T.

A different, approximated, approach[22)] is to consider f_T and τ constant across the whole depletion region. This is particularly true for deep traps since in those cases electrons have a large chance to be trapped, and the probability for an electron to be emitted from the trap center shows a small sensitivity to the bias voltage applied. As a consequence, a finite population of electrons occupy levels at the trap energy E_T within the depletion region; hence the energy difference between E_T and the quasi-Fermi level must remain constant in the depletion region, to allow the Fermi function f_T to account for the finite population of trapped electrons. This is particularly true at large reverse bias, where this concept also becomes valid for more shallow levels, as in this case both n_o and p_o are negligible. From eqs. (11)-(15) and (40) we find:

$$f_T\,\frac{g_T}{1+\left(g_T-1\right)f_T} = \frac{c_n n_o + c_p p_1}{c_n\left(n_o+n_1\right)+c_p\left(p_1+p_o\right)}. \tag{47}$$

From eq. (45), if both n_o and p_o are negligible or much smaller than n_1 and p_1 in the major part of the depletion region, f_T becomes constant within the reverse region since n_1 and p_1 do not depend on bias, as can be derived from eq. (6):

$$n_1 = N_C \exp\left(\frac{E_T-E_C}{K_B T}\right) \qquad p_1 = N_V \exp\left(\frac{E_V-E_T}{K_B T}\right). \tag{48}$$

With this simplified assumption $\overline{v_{gndr}^2}$ reduces to[22), 23), 24)]:

$$\overline{v_{gndr}^2} = \left(\frac{e}{\varepsilon}\right)^2 \frac{f_T\left(1-f_T\right)g_T}{\left[1+\left(g_T-1\right)f_T\right]^2}\,\frac{N_T}{LZ}\,\frac{4\tau}{1+\left(\omega\tau\right)^2}\,\frac{W^3}{3}. \tag{49}$$

Again, by applying eq.(A.10) and eq.(A.13) of appendix B we obtain:

$$\overline{v_{gndr}^2} = \left(\frac{e}{\varepsilon}\right)^2 \frac{f_T(1-f_T)g_T}{[1+(g_T-1)f_T]^2}\frac{N_T}{LZ}\frac{a^3}{3}\left[\frac{V_{bi}-V_G}{V_P}\right]^{3/2}\frac{4\tau}{1+(\omega\tau)^2}$$
$$= \left\{\left(\frac{e}{\varepsilon}\right)^2 \frac{f_T(1-f_T)g_T}{[1+(g_T-1)f_T]^2}\frac{N_T}{LZ}\frac{a^3}{3}\frac{4\tau}{1+(\omega\tau)^2}\right\}\left[1-\frac{L}{qn_{no}\mu Za}\frac{I_{DS}}{V_{DS}}\right]^3. \qquad (50)$$

This equation can be rearranged to give a form similar to eq. (46):

$$\overline{v_{gndr}^2} = \frac{f_T(1-f_T)g_T}{[1+(g_T-1)f_T]^2}\frac{N_T}{n_{no}}\frac{8}{3}\frac{eV_P}{C_G}\frac{\tau}{1+(\omega\tau)^2}\left[1-\frac{I_{DS}}{2V_P g_m}\right]^3, \quad C_G = \frac{\varepsilon LZ}{a}. \qquad (51)$$

The last result shows a direct dependence of the input-equivalent noise on the chosen working condition, I_{DS}. As expected, the gate noise due to G-R centers present in the depletion region is bias dependent, and is minimized when the depletion region is at its minimum width, either at V_G=0 V, or at large I_{DS}. Nevertheless in almost all the standard working conditions adopted I_{DS} is much smaller than $2V_P g_m$ so that the G-R noise coming from the depletion region can be considered bias independent. In eq.(51) the ratio of the concentration of the trapping centers to the concentration of the donor doping profile is proportional to measurable coefficients, once the terms containing the Fermi functions can be quantified, as will be shown in the following sub-sections. The noise is directly proportional to the concentration of trapping centers, as these are the only source of charge within the depletion region.

Eq. (51) is not adequate to describe the G-R noise due to shallow levels. It was derived assuming f_T and τ constant and equal to the value they assume in the deep depletion region where, in the Fermi function, eq. (47), n_o and p_o are completely negligible. In this situation f_T can never be considered comparable with its maximum value, 0.5, since the term $c_p p_1$ cannot take values comparable to $c_n n_1$ for a shallow level (see eq. (48)) unless c_p is unrealistically large. To address the inadequate approximation of eq. (51) for shallow levels and the unwieldy complexity of eq. (46) we have introduced a new approximation that takes care of both cases. Let's perform the integral of eq. (44) to be integrated over the interval (0,W) and consider also the theorem of the weighted average for integrals which states that for a given product function f(x)g(x) to be integrated over (a,b), there exists a point $c \in (a,b)$ such that $\int_a^b f(x)g(x)dx = f(c)\int_a^b g(x)dx$, if g(x) does not change sign within the interval of integration. By substituting $f(x)=f_T(1-f_T)\tau/[1+(g_T-1)f_T]^2/[1+(\omega\tau)^2]$ and $g(x)=(x-W)^2$ we get:

$$\overline{v_{gndr}^2} = \left(\frac{e}{\varepsilon}\right)^2 \frac{f_{Tc}(1-f_{Tc})g_T}{[1+(g_T-1)f_{Tc}]^2}\frac{N_T}{LZ}\frac{4\tau_c}{1+(\omega\tau_c)^2}\frac{W^3}{3}, \quad c \in (0,W). \qquad (52)$$

Or:

$$\overline{v_{gndr}^2} = \frac{f_{Tc}(1-f_{Tc})g_T}{[1+(g_T-1)f_{Tc}]^2}\frac{N_T}{n_{no}}\frac{8}{3}\frac{eV_P}{C_G}\frac{\tau_c}{1+(\omega\tau_c)^2}\left[1-\frac{I_{DS}}{2V_P g_m}\right]^3, \qquad c\in(0,W),\ C_G=\frac{\varepsilon LZ}{a} \tag{53}$$

This equation does not provide much data from a mathematical point of view, since to evaluate it we must know the point *c* within (0,W) where the necessary quantities are calculated. Nevertheless it is very useful from an experimental point of view. From eq. (47) we see that for every kind of trap (shallow or deep) having energy level smaller than the dopant energy level, there exists a temperature and a position starting from the channel side of the depletion region, at x=W, going toward the gate side of the depletion region, at x=0, where n_o takes a value (see the list of symbols in **Table 1**) that allows f_{Tc} to be equal to 0.5. This is evident if we consider that at x=W, n_o is of the order of $N_d>n_1$ for temperatures lower than the temperature at which the Fermi level within the channel is larger than E_T, and at x=0 n_o is negligible. Mathematically:

$$\frac{n_o}{n_1} = \exp\left(\frac{E_F-E_T}{K_B T}\right). \tag{54}$$

At the position and temperature at which E_F equals E_T the value of f_{Tc} approaches its maximum, resulting in the following sistuation ($p_0\approx p_c\approx 0$):

$$f_{Tc}(1-f_{Tc}) \approx \frac{(c_n n_{oc})(c_n n_1)}{[c_n n_{oc}+c_n n_1]^2} \approx \frac{1}{2} \qquad \tau_c \approx \frac{1}{2c_n n_1}. \tag{55}$$

A similar expression can be derived if $p_1>n_1$.

In a temperature interval approaching its maximum f_{Tc} has a small dependence on temperature and on the time constant τ_c. A very robust way to investigate this condition is to plot eq. (53) when $\omega\tau_c<<1$, measured at different temperatures, with respect to the time constant τ_c. If the result is found linearly dependent on τ_c, this indicates that the Fermi function is close to 0.5. This can assure us that the G-R noise we are investigating is produced by a single G-R process. In addition, from eq. (53) it is possible also to extract information about the concentration of the trapping centers, once the other, static, measurable parameters are known.

If the traps responsible for the noise under investigation are the conductivity dopants the condition of eq. (55) has a very small probability to be satisfied at very low temperature (eq.(54) when $E_T=E_d$). Hence f_{Tc} for dopants can be considered negligible, like also the generated noise in the depletion region, for most of the temperatures of interest.

Equations (46), (51) and (53) are valid only in the saturation region of transistor operation. The extension of their validity to the linear region is not considered here. In first approximation it can be derived by substituting V_{DS} with $|V_{GS}|$.

2.3.2 Gate noise due to G-R center present in the channel region

In the channel region the noise is due to the fluctuation of the charge carriers in the conduction band. For this case the quasi-Fermi level is constant in the channel and coincides with the Fermi level because the bias does not change the energy profile: the current in the channel is due only to drift. This consideration is described by the following expression:

$$\frac{\overline{\Delta I_D^2}}{I_D^2} = \frac{\overline{\Delta n_v^2}}{n_v^2}; \tag{56}$$

which is equivalent to a voltage noise on the gate of:

$$\overline{v_{nch}^2} = \left(\frac{I_D}{g_m}\right)^2 \frac{\overline{\Delta n_v^2}}{n_v^2}. \tag{57}$$

As it will be evident below, the traps in the channel have negligible effect compared to the corresponding traps in the depletion region, except for the very shallow ones at very low temperatures. We therefore concentrate on the donor levels. Using eqs. (41) and the definitions of Appendix B we get the following expression valid for dopant traps (an equivalent equation can be easily derived for a generic trap level):

$$\begin{aligned}\overline{v_{nch}^2} &= (V_{GS}-V_T)^2 f_d(1-f_d)\frac{g_d}{[1-f_d+2g_d f_d][1+(g_d-1)f_d]}\frac{N_d}{n_{no}^2}\frac{4\tau_c}{1+(\omega\tau_c)^2}\frac{1}{(a-W)LZ} \\ &= (V_{GS}-V_T)^2 f_d \frac{g_d}{[1-f_d+2g_d f_d]}\frac{4\tau_c}{1+(\omega\tau_c)^2}\frac{1}{(a-W)LZ}\frac{1}{n_{no}}\end{aligned}. \tag{58}$$

Even for this situation we can give a compact form, equivalent to eq. (55). Let's start to consider the Lorentzian time constant τ_c that, for donor dopants, can be expressed as (see **Table 3**):

$$\tau_c = \frac{1}{c_n(n_1+2n_o)} = \frac{f_d}{c_n N_d\left(1-f_d^2\right)}. \tag{59}$$

Using again the results of Appendix B we arrive at the final expression for the channel noise:

$$\overline{v_{nch}^2} = 4e\frac{V_{GS}-V_T}{C_G}\frac{g_d f_d^2}{[1-f_d+2g_d f_d]\left[1-f_d^2\right]}\frac{1}{c_n N_d}\frac{1}{1+(\omega\tau_c)^2}. \tag{60}$$

The last term of eq.(60) can be approximated to one in almost all our measurements since the Lorentzian frequency corner is much larger than the instrumentation bandwidth limit (52 KHz). When measurable this noise looks like white noise even though the mechanism responsible for it is the G-R noise from dopants.

The channel noise is a measure of the Fermi function. Even for this case the expression for the gate voltage depends on the working point. Its contribution is minimal when the conducting channel is thin, at small drain current, or when V_{GS} is close to V_T.

2.3.3 The overall G-R gate noise

It must be pointed out that the total input noise is the sum of the two calculated contributions, the one coming from the depletion region and the one coming from the channel region:

$$\overline{v_{ntot}^2} = \overline{v_{ndr}^2} + \overline{v_{nch}^2} \,. \tag{61}$$

Nevertheless since at every selected temperature only a restricted species of traps contribute to the G-R noise, in the above equation it is almost always verified that only one of the two mechanisms dominates.

For instance, for a deep or shallow trap in the depletion region at the temperature where it shows its maximum effect, the resulting Lorentzian time constant is much larger than the one generated by the corresponding trap located in the channel region. From **Table 3** and eq. (8), with n_o negligible in the depletion region, the ratio of the Lorentzian time constants of the channel and of the depletion region due to a donor trap is proportional to n_1/N_d. This ratio is negligible as long as $N_d >> n_1$, which happens for deep level traps. The two time constants should approache each other for shallow traps, or when N_d approaches n_1, a condition accomplished at very low temperatures. Nevertheless eq.(55) is hardily satisfied at very low temperature and τ_c is very large since hole generation is a very rare process for shallow donors (electron capture from the conduction band is highly inhibited in the depletion region). The effect stems from the fact that the Fermi level in the depletion region is close to the trap energy level when the maximum noise effect is measured, while it is always closed to the dopant's energy level in the channel.

The evaluation above applies also to the study of G-R noise generated by the dopants themselves as explained in the previous sub section. In this case the dopant levels inside the depletion region are empty down to very low temperatures, where the freeze-out occurs, since the generation of holes from that energy level is very difficult. The term $f_{Tc}(1-f_{Tc})$ is therefore negligible in comparison to the competitive term inside the channel region.

3 THE MEASUREMENT APPARATUS

3.1 The environment for room temperature characterization

JFET processes optimized for room temperature operation have been measured from -60 ^{O}C to +70 ^{O}C. This temperature range was found adequate for the study of the deep level traps responsible for the LF region of the noise spectra. A temperature chamber, VT7004 by Vötsch, was used for controlling the temperature of the device under test. Measurements have been made simply by putting the whole preamplifier inside a metallic box shielded with a

sheet 0.1 mm thick of SKUDOTECH®[35], a special metal alloy designed for having strong magnetic field rejecting properties. Shielding was necessary to avoid the interference coming from the fan coil present inside the temperature chamber.

3.2 The cryogenic setup

The cryogenic measurement setup has been especially designed to eliminate microphonics at low frequencies. For this reason the measurement system was designed without using mechanical pumps for cooling, stabilizing temperature or maintaining a vacuum environment around the DUT.

The DUT is put at one end of a stainless steel tube of 10 mm diameter. Inside the tube are wires that connect the DUT and diagnostics to the room temperature second stage located at the other end of the tube. The DUT is surrounded by an aluminum cylinder, which is screwed on a stopper located a few cm above the DUT. Figure 5 shows a picture of the setup.

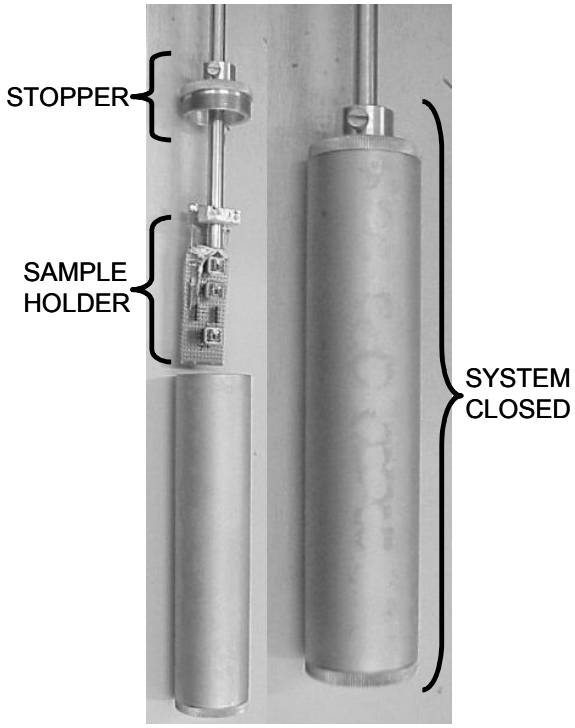

Figure 5: Photograph of the cryogenic setup implemented for minimizing microphonic effects.

The DUT is brought to a stable low temperature position by inserting the apparatus in a dewar partually filled with LN2 or LHe. The temperature is set by adjusting the distance of the DUT from the cold liquid surface inside the dewar. In this arrangement, the DUT is surrounded by a metal surface with a slightly lower temperature. This creates a cryo-pumping effect wherein the condensable components of the air inside the cylinder condense on the wall of the cylinder instead of on the DUT. Consequently ice cannot form on the DUT, and it is not necessary to create a vacuum inside the cylinder. Thus, no pumps are necessary to make

and/or maintain a vacuum. This principle of operation is opposite to that of many standard cryogenic instruments. In these situations the DUT is the coldest part of the system, so a vacuum is required for preventing any condensation of the gas on it.

The presence of ice has to be avoided since it can deteriorate the noise performances. At LF, when measuring parallel noise or leakage currents, the presence of ice can add even more disturbances. On the other hand the absence of any pump or compressor for creating and maintaining the cryogenic temperature is by far the more important benefit to the LF noise measurements, as in this case microphonics and electromagnetic interferences induced by the vibration coming from motors motion is avoided.

Since the power dissipated by the DUT and its associated bias circuitry is small (~10 mW), this temperature setting procedure has been shown to be very stable. Stability within a few tens of mK are readily obtained over periods of about one hour. Over the time intervals required for a measurement (typically 15 minutes) no significant temperature variation has been seen, as long as the dewar was not too empty or too full.

3.3 The measurement configuration

Characterizations of transistors have been made using two different set ups. In the first case JFETs were operated in a temperature range around room temperature. A pair of selected JFETs formed the differential input stage of the amplifier APRE in the schematic diagram of **Figure 6**.

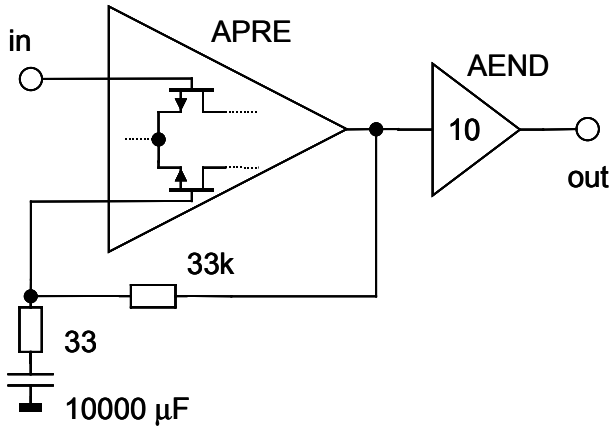

Figure 6: Schematic diagram of the second stage preamplifier used for noise measurements.

This amplifier is similar to the one described in[36]. The amplifier gain has a low frequency cutoff whose –3 dB point is 0.5 Hz. The flat band voltage gain is 1000 V/V. The amplifier output gain is further increased by a factor of 10 by the additional stage AEND. The contribution to the input noise of APRE coming from the circuit elements that follow the JFETs pair in APRE has been found negligible. The feedback contributes to the series noise mainly due to the thermal noise of the 33 Ω resistor, 0.74 nV/√Hz at 300 K. This can be subtracted out of the experimental measurements. The configuration of **Figure 6** was chosen because it was also used as the second stage of amplification for the JFET located at

cryogenic temperature, as shown in **Figure 7**. This set up was found to be very insensitive to microphonism and uses the same configuration as the bolometer readout circuits.

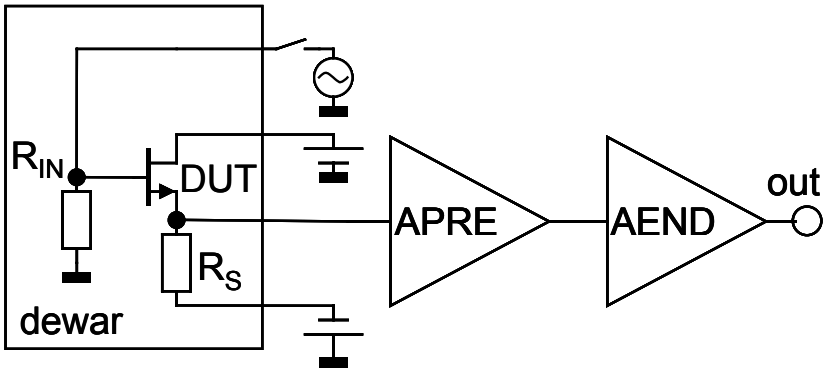

Figure 7: Schematic diagram of the cold JFET readout.

As shown in **Figure 7** the signal of the JFET DUT, held at cryogenic temperature, feed into APRE. The only contribution to the noise coming from the second stage APRE is its series noise that, due to the configuration adopted, can be measured in a very accurate way and can be removed from the overall noise measured. The DUT located at cryogenic temperature is biased in the simplest possible way: common drain configuration, **Figure 7**. This configuration has many benefits. It is self-biased, so it is not necessary to adjust the electrical parameters when the temperature changes. The gain from the input gate and the source, at its output, is closed to one. Calibration of the gain is made by injecting a signal at the input gate. The transfer function obtained in this way is the same as that of the series gate noise. Once the transfer function has been measured, the input gate of the DUT is connected to ground with the 50 Ω resistor R_{IN}, minimizing pick-up noise. The APRE is connected to the source of the cold JFET under test, with a link length of about 1 m. Since the source of the DUT is a low impedance node, microphonism is minimized. The biasing resistor at the DUT source, R_S, is held at cryogenic temperature close to the DUT, to make its thermal noise contribution negligible.

3.4 Measurement procedure

For both kinds of configuration, an HP35670A spectrum analyzer is used to read the output of the system. For each temperature setting the procedure starts with the measurement of the transfer function, which is the ratio between the output voltage of the system and the injected input signal, white noise. The second step consists of removing the input signal and measuring the system noise. The floor noise of the apparatus is then subtracted from this measurement. For room temperature JFET characterization the floor noise consists of the thermal noise of the feedback resistors. For cold temperature JFET characterization the floor noise is that of the whole APRE. For both cases the result is divided by the transfer function, to refer the noise to the input. The noise has been measured in the frequency span 1 Hz - 52 KHz, and it is represented in a log-log scale. The HP35670A measures the power spectrum using the Fast Fourier Transform, which is an algorithm that operates in the linear

scale time-frequency. To obtain precise mathematical analysis, it is necessary to have the same number of points per decade in frequency. To this aim we have performed one measurement for every frequency decade, and then concatenated the data. So each noise spectrum consists actually of 5 measurements: the first with the instrument bandwidth limited to 10 Hz, the second to 100 Hz, the third to 1 KHz, the fourth to 10 KHz and the last to the full span of 52 KHz. The same steps are performed with the measurement of the transfer function. In this way a very precise representation of the noise is obtained in the whole range of frequency investigated, easily allowing the study of the trap behavior with temperature.

The described approach of measuring the noise spectra versus temperature[37), 38), 39)] is different from that used in many previous experiments[34), 40), 41), 42), 43), 44), 45)]. In those cases the G-R noise was extracted from noise measurements performed in a narrow frequency span around a chosen measurement frequency, ω_M, looking for a maximum with temperature. This approach has been found to be inaccurate at low temperature. Following this procedure the shape around the maximum as a function of temperature of the noise in eq. (53) is considered to be dominated mainly by the term $\tau/(1+(\omega_M\tau)^2)$, hence a maximum should be obtained when the measurement frequency, ω_M, equals the Lorentzian frequency $1/\tau$. Actually, in eq. (53), the maximum should instead considered proportional to $f_T(1-f_T)\tau/(1+(\omega_M\tau)^2)$, a more complicated function of temperature, that does not necessary have a peak at $\omega_M=1/\tau$.

We measured the noise spectrum at a selected temperature, finding the Lorentzian frequency $1/\tau$ from the roll off of the spectrum. This measurement is independent of the noise amplitude, and also independent from $f_T(1-f_T)$. In addition, the amplitude of the flat part of the Lorentzian component of the noise, the region where $\omega<<1/\tau_T$, which we can now discern, is proportional to the product $f_{Tc}(1-f_{Tc})\tau_c$ (see sub section 2.3.1). After making a temperature scan, we added a further analytical step by plotting the amplitudes of the measured flat part of the Lorentzian components as a function of the Lorentzian frequencies. For a robust interpretation of the noise, we look for the region where this curve is linearly dependent on τ_c. This condition is fulfilled close to the maximum of the function $f_{Tc}(1-f_{Tc})$, where the temperature dependence of it has the minimum sensitivity. Therefore, our approach allows us to get an additional degree of freedom. The two interesting parameters to be extracted are the trap cross-section, which is proportional to the Lorentzian frequency, and the trap density, which is proportional to the flat part of the Lorentzian noise contribution. In our procedure these two quantities are now two measurement parameters.

4 THE EFFECTS OF DEEP LEVEL TRAPS ON THE NOISE

The noise is dependent on the quasi-Fermi level. In this case the dominant noise source is localized in the depletion region (see eq.(51)) and the largest contribution to the noise is from those traps with an energy level close to the quasi-Fermi level, for which $f_T(1-f_T)\approx 0.25$. At room temperature this happens for traps with activation energy close to the middle of the band gap. To study the effect of G-R noise around room temperature we have selected two very low noise JFET processes: the dual 2SK146 from Toshiba and the dual SNJ3600 from Interfet. We have measured their noise in the temperature range –60 ^{O}C to 70 ^{O}C using the set

up described in sub section 3.1. Each of the JFETs was connected as the input device of the preamplifier of **Figure 6**. The whole preamplifier was then put inside the temperature chamber. The temperature was stepped by about 10 ^{O}C between the indicated limits. In **Figure 8** the series noise over the full temperature range for each of the dual 2SK146 JFETs is shown in a 3D-plot, after the noise of the feedback resistor has been subtracted. Each JFET was operated at I_{DS}=1 mA and V_{DS}=1 V. The presence of a trap is evident whose G-R noise starts to be present in the measured spectra from about –40 ^{O}C. As the temperature increases the noise due to this trap decreases, while the frequency of the G-R process increases. At the larger temperatures the amplitude of this G-R noise disappears and the LF noise starts to increases again, probably due to the presence of another kind of trap. In **Figure 8** a mathematical fit to each noise spectrum is superimposed. At the very beginning we tried to interpolate the noise spectra with a function given by the superposition of the effects coming from 5 traps:

$$\overline{e_J^2} = \sum_{k=1}^{4} \frac{A_{LOR\_k}}{1+\left(f/f_{LOR\_k}\right)^2} + \frac{A_{LOR}}{1+\left(f/f_{LOR}\right)^2} + \overline{e_{white}^2}, \qquad \text{where } \omega = 2\pi f,\ \tau = 1/\omega. \tag{62}$$

Since there was evidence for a single dominant trap at frequency f_{LOR} for these very low noise devices, the other first 4 G-R noise traps frequencies, f_{LOR_k}, were not determined with enough precision, mainly because they were found located at frequencies well below 1 Hz, the lower limit of the collected spectra. In this situation the fit is sensitive to the terms $A_{LOR} f_{LOR\_k}^2 \Big/ f^2$ for each frequencies f_{LOR_k}. The superimposition of the contributions of these four smaller frequencies can therefore be easily accounted for by a single term:

$$\overline{e_J^2} = \frac{A_f}{f^{esp}} + \frac{A_{LOR}}{1+\left(f/f_{LOR}\right)^2} + \overline{e_{white}^2}. \tag{63}$$

As can be seen in **Figure 8** the above interpolating function satisfactory accounts for the measured noise. To fit the spectra we have used the χ-square technique with the robust estimator[46], which allows weighting the data to be interpolated with weights proportional to a power of the inverse of the value of the data itself. This fitting algorithm was applied to the noise power measured, although in the following figures only the square root of the noise will be shown. The interpolated parameters obtained for the 2SK146 JFET are summarized in **Table 4**.

The same procedure has been adopted for the SNJ3600, operated at 5 mA of drain current and 1 V of V_{DS}. The noise versus temperature data obtained for it, together to the fit results, are shown in the 3D-plot of **Figure 9**, while the extracted parameters are listed in **Table 5**.

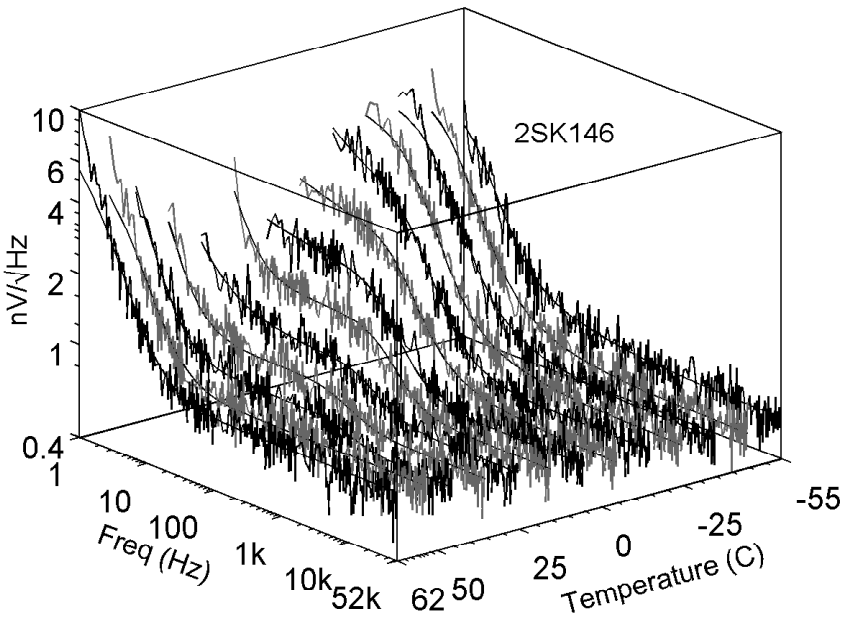

Figure 8: 3D-plot of the noise spectra measured for the JFET 2SK146. To each noise spectrum the calculated fit is superimposed.

Table 4: Parameters extracted to fit the spectra of Figure 8, the series noise of the 2SK146 JFET, according to the function of eq.(63).

A_f $[(nV)^2/Hz^{(1-Esp)}$	Esp	A_{lor} $[(nV)^2/Hz]$	f_{lor} [Hz]	White $[(nV)^2/Hz]$	temperature $[^oC]$
1.021	0.500	13.339	1.359	0.356	-55
1.822	0.647	16.771	1.980	0.312	-45
2.281	0.622	17.730	3.211	0.332	-35
2.798	0.633	18.043	4.474	0.347	-25
10.776	0.969	7.931	13.087	0.378	-15
3.335	0.573	4.579	28.517	0.345	-5
1.159	0.733	2.856	53.286	0.397	5
6.987	1.997	1.519	174.144	0.432	15
2.775	1.179	0.674	324.622	0.478	25
6.084	2.000	0.460	426.302	0.507	35
15.691	1.913	0.276	1365.288	0.509	45
6.815	1.444	10.873	1.858	0.602	53
14.376	1.421	19.555	1.894	0.621	62

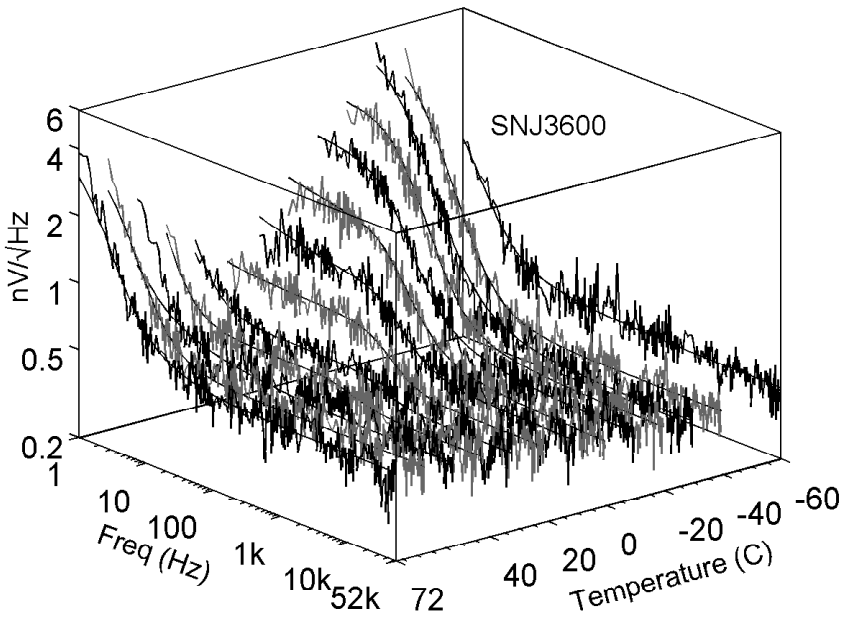

Figure 9: 3D-plot of the noise spectra measured for the JFET SNJ3600. To each noise spectrum the calculated fit is superimposed.

Table 5: Parameters extracted to fit the spectra of Figure 9, the series noise of the SNJ3600 JFET, according to the function of eq.(63).

A_f $[(nV)^2/Hz^{(1-Esp)}]$	Esp	A_{lor} $[(nV)^2/Hz]$	f_{lor} [Hz]	white $[(nV)^2/Hz]$	temperature [^OC]
0.222	0.511	4.752	0.838	0.176	-60
0.948	0.919	14.803	1.691	0.148	-40
1.399	0.707	19.602	2.201	0.140	-30
0.614	0.555	9.264	5.929	0.146	-20
0.991	0.510	4.616	11.174	0.149	-10
0.922	0.501	1.736	33.184	0.148	0
0.617	0.501	0.656	88.680	0.175	10
0.097	0.883	0.404	205.844	0.188	21
0.943	1.981	0.129	566.026	0.196	32
1.378	2.000	0.111	584.567	0.213	42
0.337	0.500	1.269	0.806	0.216	52
0.227	0.810	9.240	1.142	0.240	62
0.773	0.665	13.232	1.213	0.248	72

From the parameters taken from **Table 4** and **Table 5** a number of facts can be deduced. Let us start by examining the frequency behavior of the Lorentzian traps. The associated time constant is given in eq.(9). If we assume that we are close to the maximum of the product $f_{Tc1}(1-f_{Tc})$ then:

$$\tau \approx \frac{1}{2c_n n_1} \quad \text{or} \quad \frac{1}{2c_p p_1} \ . \tag{64}$$

If we make the approximation that one term in the denominator of τ dominates we face two situations. The first case is when $n_1 >> p_1$:

$$\frac{1}{\tau} \approx 2c_n n_1 \approx 4\left[\frac{2\pi K_B m_n}{h^2}\right]^{3/2}\left[\frac{3K_B}{m_n}\right]^{1/2}\sigma T^2 \exp\left(\frac{E_T - E_C}{K_B T}\right). \tag{65}$$

On the other hand, when $p_1 >> n_1$ we obtain:

$$\frac{1}{\tau} \approx 2c_p p_1 \approx 4\left[\frac{2\pi K_B m_h}{h^2}\right]^{3/2}\left[\frac{3K_B}{m_h}\right]^{1/2}\sigma T^2 \exp\left(\frac{E_V - E_T}{K_B T}\right). \tag{66}$$

We therefore expect the Lorentzian frequency to be proportional to the product of the square of the temperature and the exponential of the ratio of the energy of the trap, measured with respect to the appropriate band level and divided by the temperature. From this kind of measurement it is not possible to determine if the trap is a donor or an acceptor since for both cases the trap energy is measured with respect to the conduction band or the valence band edge, respectively, with the same final effect on the shape of the function.

The temperature dependence of the Lorentzian frequencies, f_{LOR}, with respect to the inverse of temperature is shown in the log-log plot of **Figure 10** for both the JFETs.
It is very interesting to observe that, although manufactured with different processes and by different companies, the temperature dependence of the G-R noise due to the observed traps in this temperature range is exactly the same. If we discard the Lorentzian frequencies obtained by fitting the data at the lower and higher temperatures, whose values are at the limits of sensitivity, all the parameters can be fitted by a single function that can be deduced by the above eq. (65) and (66). The fitting function used has been:

$$f_{LOR} = a\frac{1}{x^2}\left(\frac{e}{K_B}\right)^2 \exp(bx)\ [\text{Hz}], \qquad x = \frac{e}{K_B T}. \tag{67}$$

The fit is plotted in **Figure 10**, superimposed on the data. The temperatures range over which eq.(67) is applied is the one where the coefficients A_{LOR} in eq. (62) are linearly dependant on $1/f_{LOR}$. From eq. (53) it is seen that this property is satisfied by a Fermi-function which is flat in the considered temperature range, allowing us to get a better approximation of f_{LOR} that, in turn, depends in some way on the Fermi-function itself.

As can be seen, the energy of the trap (fitting parameter b) is located about 0.50 eV above the valence band or below the conduction band. This energy is typically attributed to gold acceptors. From the fitting parameter *a* it is possible to extract the order of magnitude of the cross-section σ.

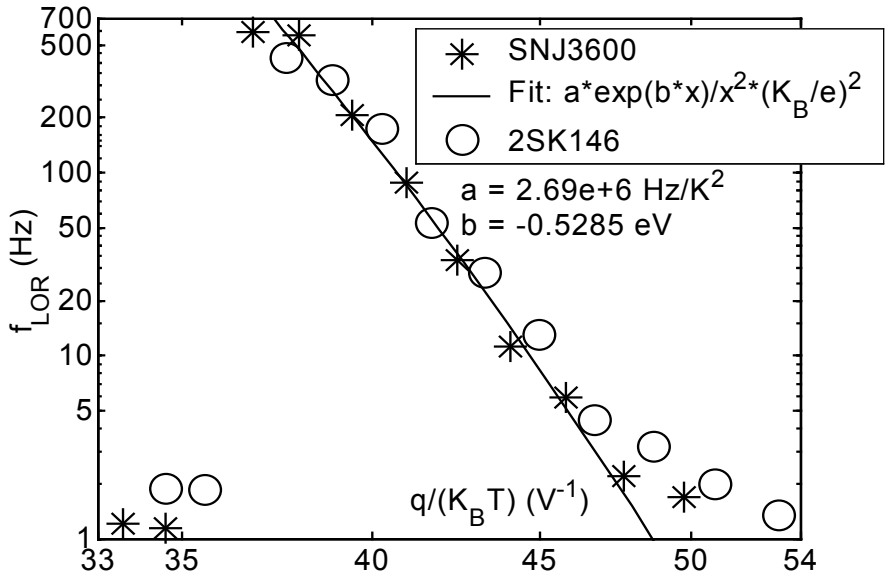

Figure 10: Log-log plot of the Lorentzian frequencies versus the inverse of the temperature for both the SNJ3600 (*) and the 2SK146 (O) JFETs.

From eq.(65) and (66) we can rearrange the terms to obtain:

$$f_{LOR} = \frac{1}{2\pi\pi} \approx 1.036\times10^{25}\frac{m_{n(h)}}{m_e}\sigma T^2 \exp\left(-\frac{\Delta E_T}{K_B T}\right)$$
$$= 1.036\times10^{25}\frac{m_{n(h)}}{m_e}\sigma\left\{\frac{1}{x^2}\left(\frac{e}{K_B}\right)^2 \exp(bx)\right\} \quad . \tag{68}$$
$$\Delta E_T = (E_C - E_T) \text{ or } (E_T - E_V)$$

Equating eq.(68) to eq.(67) gives the result:

$$\sigma = a\frac{m_e}{m_{n(h)}}\cdot 9.65\times10^{-22}\ \text{cm}^2. \tag{69}$$

For the case in which the electron reduced mass is close to $0.5m_e$, σ is about 10^{-14} cm^2, using the fitting parameter *a* from **Figure 10**. For holes, which have reduced mass of about $2m_e$, the cross-section is about 10^{-15} cm^2. This is consistent with the values obtained by other studies[22), 47)].

We can also attempt to deduce the concentration of the traps responsible for this G-R noise. Starting from the expression for the G-R noise given in eq. (51), we can estimate the concentration of the trap as a function of only measured parameters and on the channel

doping profile. In eq. (51) the only parameter that it is difficult to know in the depletion region is the Fermi function. Let us suppose in advance that it is quite constant and equal to 0.5 in the temperature range considered. If this were true, as described above, we would expect the amplitude of the Lorentzian noise to be linearly dependant on the Lorentzian time constant τ. In **Figure 11** the plot of the Lorentzian amplitudes, A_{LOR}, versus the inverse of Lorentzian frequencies is plotted for the 2SK146, after the parameters extracted at the lower and larger temperature have been excluded. From the figure it is possible to see that the behavior is almost linear and, therefore, the Fermi function can be assumed to be almost constant. From eq.(63) and eq.(51) we can approximate:

$$A_{LOR} \approx \frac{N_T}{n_{no}} \frac{V_P}{C_G} \cdot 1.3\times10^{-20} \frac{1}{f_{LOR}} V^2/Hz. \tag{70}$$

The coefficient indicated in the above equation is the mean value between the one that results from setting the degeneracy factor g_T equal to 2 (donor traps) and setting g_T equal to 4 (acceptor traps). The ratio for the two cases is about 40 %.

For the 2SK146 V_P is about 1.1 V and the input capacitance (for the fully depleted condition) is close to 65 pF[48)]. Using eq. (70) and the slope extracted from **Figure 11** we calculate that the ratio N_T/n_{no} is about 4×10^{-7}. If we consider that the typical doping concentration for a JFET channel is of the order of 10^{16} atoms/cm^3, we can estimate the concentration of the G-R traps at 0.50 eV in the 2SK146 to be about 4×10^9 atoms/cm^3.

The same estimation has been made also for the SNJ3600 (see the fit of Figure 12). This device has V_P of about 2 V and input an capacitance of about 500 pF[48)]. Consequently the ratio N_T/n_{no} has the order of magnitude of about 10^{-6}, or concentration N_T of about 10^{10} atoms/cm^3 for the case that N_d is of the order of 10^{16} atoms/cm^3.

In **Table 6** the extracted parameters for both the Silicon JFETs 2SK146 and SNJ3600 are summarized.

Table 6: Extracted parameters for the traps responsible of the G-R noise for the 2SK146 and SNJ3600. The terms a and b are the parameters extracted from the fitting function given in eq. (63). In the last column in parenthesis is the energy measured from the nearest band edge. The levels are donors except those indicated with the letter A.

	V_P/C_G [V/pF]	**N_T/N_d**	**a of eq. (67) [Hz/K^2]**	**|b| of eq.(67) (trap energy) [eV]**	**σ [cm^2]**	**Trap candidates**
2SK146	1.1/65	4×10^{-7}	2.22×10^5	0.53	1×10^{-14}	Mn (0.53), Cd (0.55), Au (0.54 A), Co (0.53A), Cu (0.53), Fe (0.51), O (0.51)
SNJ3600	2/500	1×10^{-6}	5.85×10^6			

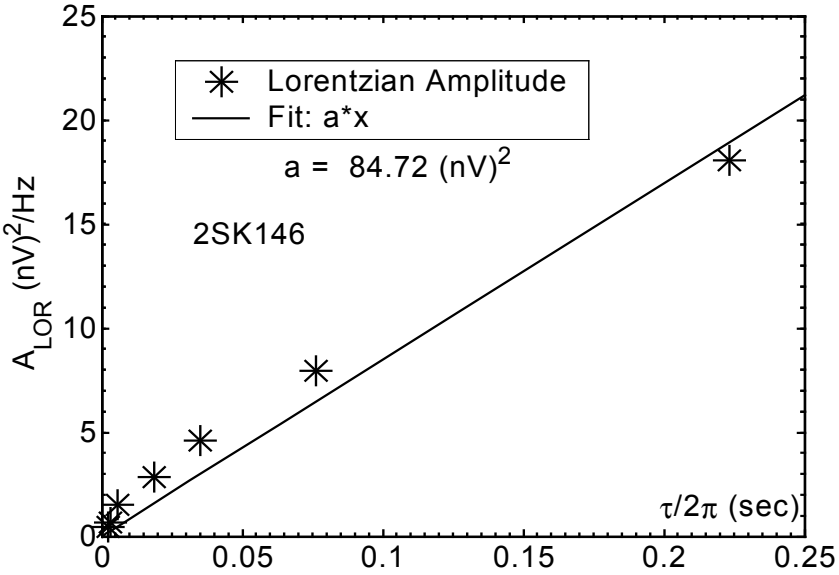

Figure 11: Amplitude of the Lorentzians with respect to the Lorentzian time constant for the JFET 2SK146.

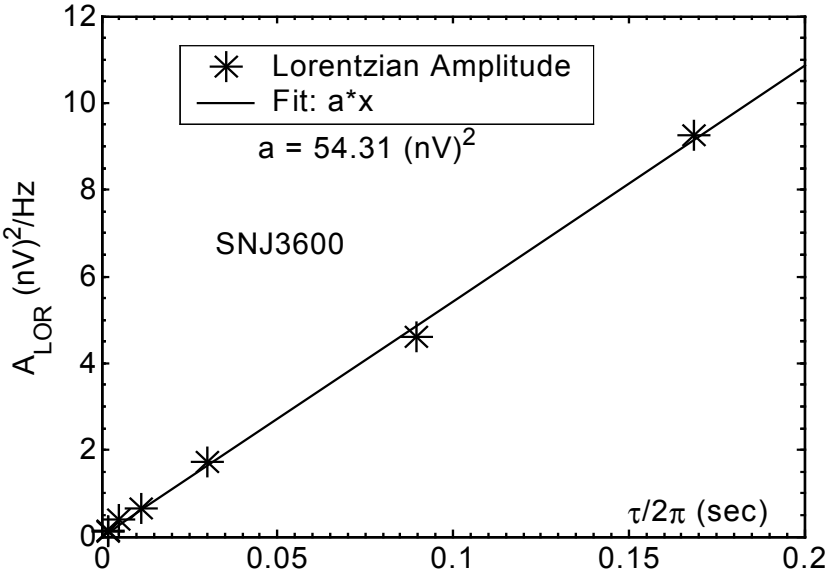

Figure 12: Amplitude of the Lorentzians with respect to the Lorentzian time constant for the JFET SNJ3600.

5 THE EFFECTS OF SHALLOW LEVEL TRAPS ON THE NOISE

The shallow level traps have the maximum effects on the G-R noise at lower temperatures than the deeper traps. Reducing the temperature reveals their presence. We have selected a very low noise Si JFET process especially designed for low temperature

operation[49)]. We scanned the temperature in two ranges: from 80 K to about 150 K and from 80 K down to 14 K. In this section we will shown the results for the first situation. We have measured different JFET transistor types from Moxtek. In Figure 13 the 3D-plot of the JFET MX16RC noise is shown measured in the temperature range from 95 K to 150 K.

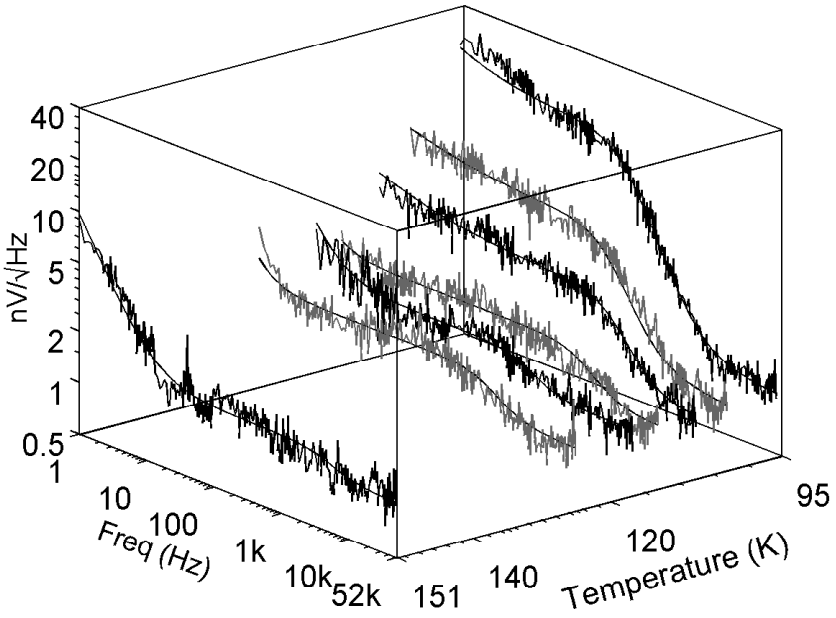

Figure 13: 3D-plot of the noise spectra measured for the JFET MX16. To each noise spectrum the calculated fit is superimposed.

The presence of a trap is evident through its effect in the LF region of the spectra over the temperature range 95 K to 125 K. Another device type for which evidence of a shallow trap is visible is the MX17-OLD shown in Figure 14. This device has been labeled OLD to distinguish it from another device of the same type received later in our lab. The interesting fact is that for this latter sample it was possible to see the effect due to another kind of trap, as can be seen in Figure 15. In these three figures the fitting curves have been added, calculated using eq. (63). The extracted parameters are listed in Table 7, Table 8 and Table 9, respectively.

We have also extracted the parameters of interest from the above measurements. In Figure 16 the coefficients A_{LOR} of eq. (63) has been plotted as a function of the inverse of the Lorentzian frequencies. As can be seen, over the temperature range considered, a linear fit works well. In Figure 17 we plotted the Lorentzian frequencies versus the inverse of temperature. The fit has been calculated for the temperature range found in Figure 16.

The summary of the parameters extracted from the measured noise is given in Table 10. These three JFETs have shown a moderately small noise. The concentration of the traps has been found to be very small compared to the donor concentration. The smaller traps concentration has been found for the MX17-NEW to be about 2×10^{10} atoms/cm^3, once N_d has been assumed to be equal to 10^{16} atoms/cm^3.

Table 7: Parameters extracted to fit the spectra of **Figure 13**, the series noise of the MX16RC JFET, according to the function of eq.(63).

A_f $[(nV)^2/Hz^{(1-Esp)}]$	Esp	A_{lor} $[(nV)^2/Hz]$	f_{lor} [Hz]	white $[(nV)^2/Hz]$	temperature $[^OC]$
274.1893	0.724842	258.6505	249.9027	1.243669	95.6
45.41338	0.500001	43.4201	757.4424	1.227896	102.9
15.30944	0.500001	13.42449	2620.481	1.203175	107.4
2.090446	1.997035	3.651591	3991.802	1.327045	112.9
10.60232	1.591671	2.179279	1339.226	1.413924	116.6
3.999812	1.99998	2.629386	2682.975	1.313125	124.9
89.51484	1.485001	0.928339	4855.303	1.091414	151

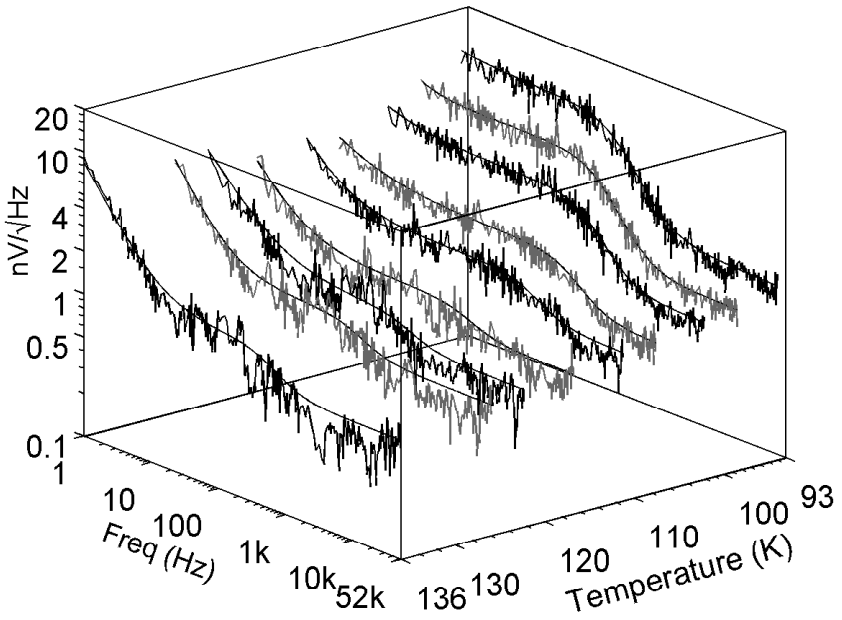

Figure 14: 3D-plot of the noise spectra measured for the JFET MX17-OLD. To each noise spectrum the calculated fit is superimposed.

The cross-section calculations follows the same rule of the previous sub section, applying eq. (69). In Table 10 some possible candidates for the found traps are given. As can be seen, around 100 K the difference between the trap energy and the band edge is around 0.1 eV.

Another transistor of this series had even better performances. In Figure 18 the 3D-plot of the noise of the MX11CD is given for the temperature range 90 K to 140 K.

As can be seen at the optimum temperature of operation for the LF noise, about 110 K, this transistor has a negligible LF noise. For the MX11CD it was not possible to find the presence of any kind of traps in this temperature range. Many other devices of the MX process have shown these very excellent characteristics[50].

Another interesting property of the MX11CD is that its pinch-off voltage is close to 5 V. This feature made this device attractive for testing at much lower temperature, as will be illustrated later.

Table 8: Parameters extracted to fit the spectra of Figure 14, the series noise of the MX17-OLD JFET, according to the function of eq.(63).

A_f $[(nV)^2/Hz^{(1-Esp)}]$	Esp	A_{lor} $[(nV)^2/Hz]$	f_{lor} [Hz]	white $[(nV)^2/Hz]$	temperature [^oC]
20.51272	0.500018	76.41827	186.5633	2.445714	93.8
16.44479	1.999997	38.03855	417.1653	1.61165	98.3
11.88086	0.874069	17.2747	884.7388	1.381547	102
10.63889	0.954338	5.232099	2459.016	1.030719	107.4
18.14603	1.376838	2.742988	2051.961	0.971462	111.1
15.99001	1.690116	1.135452	251.222	0.748086	116.6
32.74225	1.196739	1.035825	809.3682	0.585964	122.1
38.90181	1.762728	1.233236	458.2628	0.45369	125.8
97.92307	1.701299	1.42891	415.5337	0.2542	136

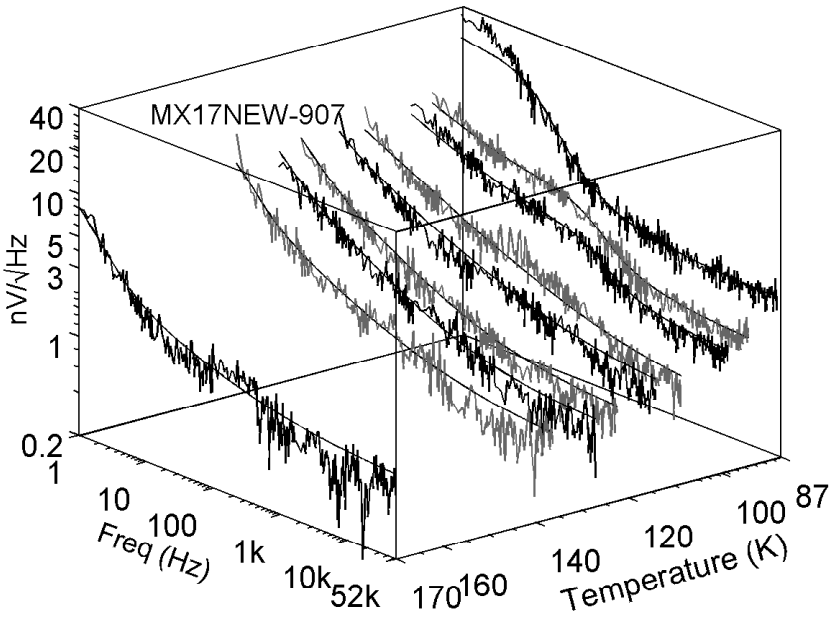

Figure 15: 3D-plot of the noise spectra measured for the JFET MX17-NEW. To each noise spectrum the calculated fit is superimposed.

6 ELECTRIC FIELD EFFECTS AT LOW TEMPERATURES AND OPERATING CONDITIONS

In all the previous sections we have neglected any possible field effect on the energy profile of the electrons inside the transistors, although the applied electric field does introduce a

small perturbation of the energy profile. Another effect to be considered, as the temperature is lowered, is electron freeze-out, or more accurately, carrier trapping at dopant sites. This effect can limit the performance of the transistor if some technological precautions are not taken.

A JFET to be operated at low temperature needs an important requirement to be satisfied. From eq. (A.15) we see that the maximum current that can flow between drain and source is obtained when V_{GS}=0 V, or:

$$I_{DS} = e n_{no} Z a \mu \frac{V_{DS}}{L} \frac{1}{2} \frac{(-V_T)}{V_P}. \qquad (71)$$

From above it is evident that for I_{DS} to be positive V_T needs to be less than 0 V. The threshold voltage V_T can be deduced from eq. (A.11), repeated here:

$$V_T = V_{bi} - V_P = V_{bi} - \frac{e n_{no} a^2}{2\varepsilon} \quad . \qquad (72)$$

Table 9: Parameters extracted to fit the spectra of Figure 15, the series noise of the MX17-NEW JFET, according to the function of eq.(63).

A_f $[(nV)^2/Hz^{(1-Esp)}]$	Esp	A_{lor} $[(nV)^2/Hz]$	f_{lor} [Hz]	white $[(nV)^2/Hz]$	temperature [^oC]
208.0705	0.645816	355.1392	12.05176	6.919963	87.5
104.6279	0.701971	19.40413	265.4406	2.413849	93.8
110.5608	0.748147	10.39783	592.9234	1.866645	98.3
58.60346	0.629663	4.253034	1256.507	0.907616	108.3
74.02431	0.770751	2.307245	2943.952	0.852619	113.8
69.85785	0.866003	1.530011	555.2914	0.667178	122.1
58.75643	0.842512	0.946359	830.0459	0.45878	126.8
37.96675	0.756611	0.874739	777.7676	0.356048	136
75.37606	1.518874	1.489019	533.5621	0.426935	169.9

It has to be remarked that people tend to identify the threshold voltage V_T with the pinch off voltage V_P. This is a good approximation at room temperature since the difference between the two absolute quantities is about 0.6 V, the built-in voltage of the band gap of Si at 300 K. At cryogenic temperatures this approximation is not valid anymore. There are two situations to consider. At temperatures above about 70 K the carrier concentration n_o can be approximated by the doping concentration N_d in almost all situations encountered with conventional JFETs[51]. The temperature coefficient of V_T therefore coincides with that of V_{bi}, or –2 mV/^{o}C. At temperatures smaller than 70 K, n_o decreases in value and the temperature coefficient of V_T becomes even more negative, leading V_T to 0 V as the temperature lowers. For instance at 70 K V_{bi} is about 1 V, so we need $V_P \geq 1$ V, let's say 1.2 V to have V_T<0. To achieve this at room temperature it must be satisfied $V_T \leq$-0.6 V. This voltage is the minimum (in absolute value) threshold voltage that a JFET capable of working at 70 K should have at

room temperature. The pinch-off voltage, V_P, should be even larger for the JFET to work at temperatures smaller than 70 K.

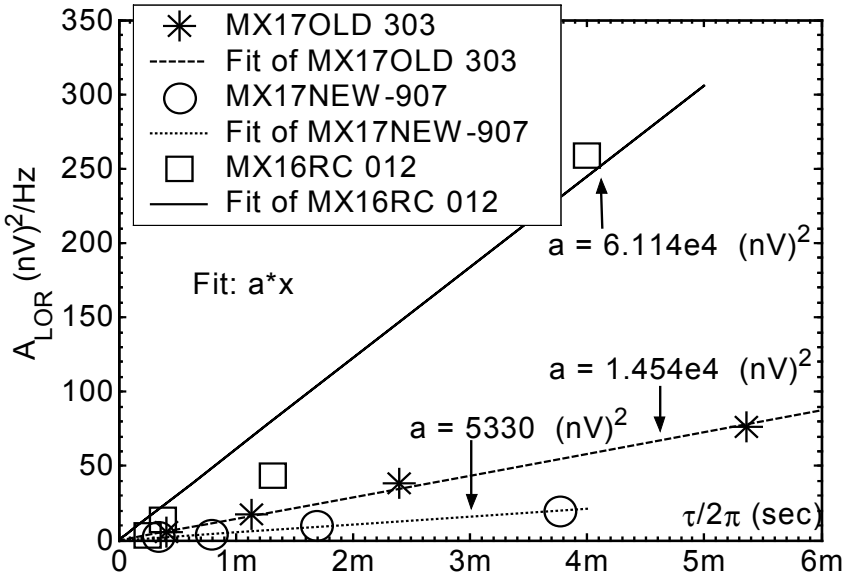

Figure 16: Coefficients A_{LOR} of eq. (63) as a function of the Lorentzian frequencies for the 3 JFETs MX16RC, MX17-OLD and MX17-NEW.

Table 10: Extracted parameters for the traps responsible of the G-R noise of the 3 JFETs MX16RC, MX17-OLD and MX17-NEW. The terms a and b are the parameters extracted from the fitting function given in eq. (63). In the last column in parenthesis is the energy measured from the nearest band edge. The levels are donors except those indicated with the letter A.

	V_P/C_G [V/pF]	**N_T/N_d**	**a of eq. (67) [Hz/K^2]**	**|b| of eq.(67) (trap energy) [eV]**	**σ [cm^2]**	**Trap candidate**
MX16RC	2.5/44	8.3×10^{-5}	2.22×10^{5}	0.1312	4.5×10^{-16}	Mg (0.11 A), Te (0.14), Fe (0.14)
MX17-OLD	4.7/22	5.2×10^{-6}	5.85×10^{6}	0.1587	1.15×10^{-14}	O (0.16), Pb (0.17 A), Be (0.17A)
MX17-NEW	4.7/22	1.9×10^{-6}	2.95×10^{3}	0.09297	5.5×10^{-18}	Ga (0.072 A), Mg (0.11 A)

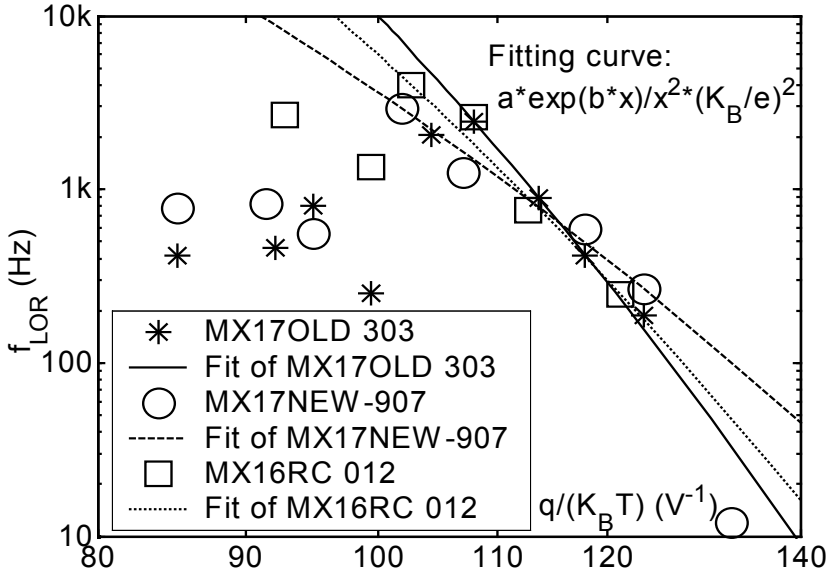

Figure 17: Lorentzian frequencies for the 3 JFETs MX16RC, MX17-OLD and MX17-NEW and the respective interpolating fits.

As can be seen in eq. (72) the designer has two degrees of freedom for increasing the pinch off voltage V_P: he can increase the doping concentration and/or increase the channel thickness a[52]. The adoption of a large thickness for a is the better choice, since it allows the designer to obtain large values of the transconductance over the input capacitance ratio. This because g_m is proportional to a, while the input capacitance is inversely proportional to a. In addition, a large thickness allows the designer to employ a small dopant concentration, obtaining a large mobility at low temperatures, since there is lower scattering from the doping atoms[53]. Furthermore, a lower channel doping lowers the gate junction capacitance because the transition from n to p type is less abrupt.

For instance, the MX11CD JFET from Moxtek has a channel thickness of 1.5 μm, from which we can estimate a doping concentration between 2 and 3 times 10^{15} atoms/cm^3, considering that its pinch off voltage V_P is between 3 V and 5 V at room temperature. The MX11CD has been found to be an excellent candidate for operation down to 14 K.

When an electric field is applied a force is given to the electrons, even if they are trapped. This force increases their potential energy. Therefore, the energy (principally thermal) needed for the electrons to escape from the trap levels becomes smaller as the electric field is increased. This effect is known as Poole-Frenkel effect[54]. We can approximate the energy profile of a trapped electron with a potential well model. As soon as the electron escapes from the trapping centers, it is subject to an attractive force proportional to the square of the inverse of the distance from the well. The resulting profile is the continuous curve of **Figure 19**. If a local constant electric field is applied, the resulting energy profile is the dashed curve shown, or:

$$U \approx -\frac{e^2}{4\pi\varepsilon r} - eEr. \tag{73}$$

The maximum of U coincides with the barrier lowering and is:

$$\Delta U_{PF} \approx -\sqrt{\frac{eE}{\pi\varepsilon}}\ eV. \tag{74}$$

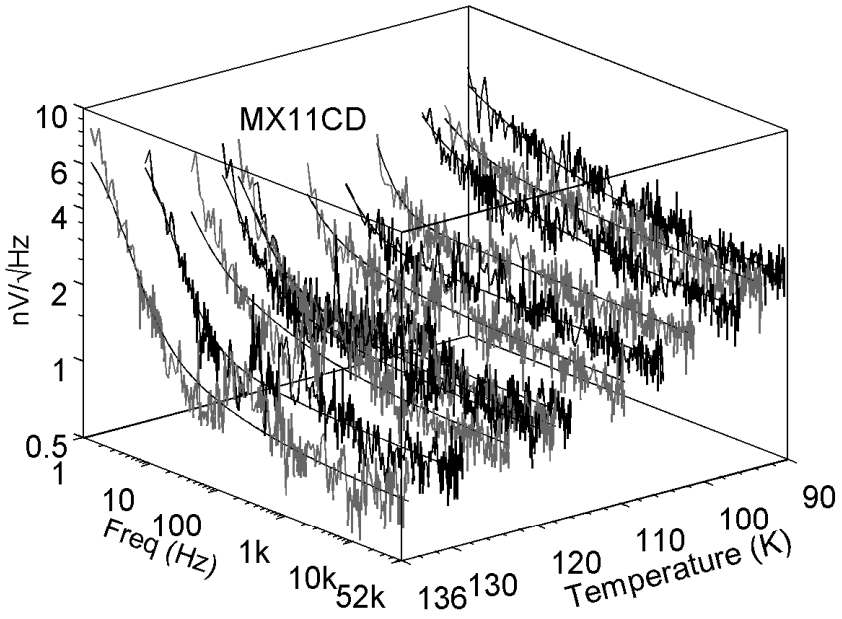

Figure 18: 3D-plot of the noise spectra measured for the JFET MX11CD. To each noise spectrum the calculated fit is superimposed.

In the depletion region the electric field applied between the gate and the channel is proportional to the distance from the gate. Substituting eq. (42) into eq. (74) we get:

$$\Delta U_{PF} \approx -\frac{e}{\varepsilon}\sqrt{\frac{n_{no}|x-W|}{\pi}}\ eV, \qquad x=0 \text{ at the gate side}. \tag{75}$$

It is very difficult to try to account for this contribution to the noise present in the depletion region, since the latter is a function of the depletion region depth and profile. We estimate here the maximum barrier lowering that is obtained at the gate side of the region, at x=0. Let's put W=αa, with α a parameter close to 1. Using eq. (A.11) ($\varepsilon \approx 12\varepsilon_o$):

$$\Delta U_{PF} \geq -\sqrt[4]{\frac{2\alpha e^3 n_{no} V_P}{\pi^2 \varepsilon^3}}\ eV. \tag{76}$$

In **Table 11** this amount is shown for a few cases. We can see that for deep level traps the possible maximum effect is small and more or less comparable to the measurement error,

while for shallow traps the effect is not totally negligible. From these considerations it is evident that the energy extracted from the noise measurements is always subjected to a systematic error, the measured value being less than the actual one.

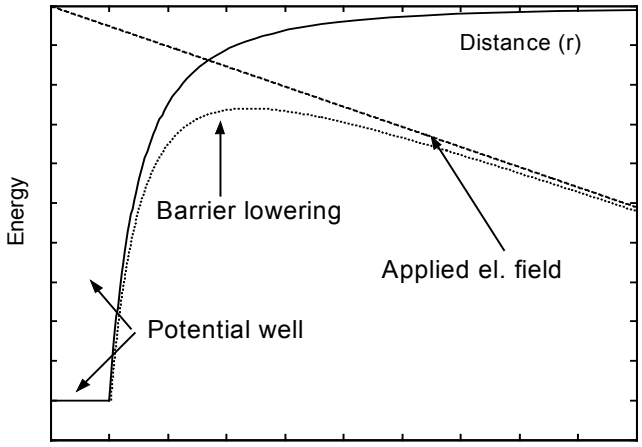

Figure 19: Energy profile of an electron close to a trapping center. The continuous curve is the case where the electron feels only the attractive force of the trap, the dashed curve is the energy profile that results when an electric field (dotted curve) is applied.

The Poole-Frenkel is able to account also for the reason Si-MOS transistors are able to work down to 4.2 K, in spite of carrier freeze-out[55]. By applying eq. (74) to the gate oxide of a MOS transistor we find that the potential energy just at the channel surface, below the oxide is:

$$\Delta U_{PF} \approx -\sqrt{\frac{e}{\pi\varepsilon}\frac{V_G}{d_{oxide}}}\ \text{eV}. \qquad (77)$$

The application of only 1 V across a thickness of 200 nm of gate oxide, d_{oxide}, generates at the channel surface an energy ΔU_{PF} of about 48 meV, enough to free electrons from donors in silicon.

Table 11: Maximum effect of the Poole-Frenkel phenomenon or trap energy reduction in the depletion region, as a function of the Pinch-off voltage and doping concentration, according to eq. (76) (parameter α=1).

V_P [V]	N_d [10^{16} atoms/cm^3]	ΔU (Poole-Frenkel) [meV]
1	1	-48
	0.1	-27
5	1	-72
	0.1	-40

The more evident contribution of the Poole-Frenkel can be seen in studying the G-R noise given by dopants inside the channel of a Si-JFET at low temperatures. In this case it is possible to make a precise estimation, since the Fermi level inside the channel is not affected by the applied field. This is because the channel is neutral and the current is due to drift. The electric field is therefore constant and ΔU_{PF} is given by:

$$\Delta U_{PF} \approx -\sqrt{\frac{e}{\pi\varepsilon}\frac{V_{DS}}{L}}\ \text{eV}. \tag{78}$$

For a gate length L of 1 μm the expected energy drop is about 22 meV when the applied voltage across the channel is 1 V, while for 2 μm of gate length the expected lowering is 15.5 meV. This effect is extremely small, but must be compared with the energy of the dopants typically used in Si, which is 45 meV below E_d.

We do not consider in this paper the application of electric fields larger than the one considered above, which would lead to complete free-up of charge. This operating range was outside our experimental requirements. This subject deserves further study in a future paper.

7 DONOR DOPANTS AS A SOURCE OF G-R NOISE

Every type of trapping center, donor or acceptor, is a source of noise. Whether this noise is large or not depends on the time constant of the process, which is tied to the Fermi level and to the Fermi function. This rule applies also to dopants inside the channel of the transistor. Since their energy level is close to the conduction band the time constant of the trapping/de-trapping process is very short at ordinary temperatures: in other words, the donor dopants are ionized. Therefore, G-R noise from dopant atoms is not measurable at room temperature. The time constant associated with this type of trap remains small, down to less than 50 K. The noise effect is measurable due to the exponential increases of its amplitude as the temperature drops (eq.(60)). For this reason for a long time it was believed that this 'anomalous' noise increase was due to high electric field or hot-electron effects[56), 57)]. Only after the work of Van der Ziel[32)], was the source of this noise understood.

G-R noise around and below 10 K has already been investigated with Si-MOS transistors[58), 59)] which, as seen above, are able to work in this temperature range. Nevertheless, in MOSFETs the electrons in the channel have an energy profile different than in JFETs. For this reason, we tried to investigate the behavior of a Si-JFET at these very low temperatures of operation. As seen in section 6 we found a candidate for this experiment in the MX11CD JFET transistor from Moxtek, which has a large pinch-off voltage coming from the large thickness of its conducting channel.

The only method used so far for investigating G-R noise from dopants was to measure the time constant of the process. We will show below that this is not necessary if an accurate mathematical model is adopted for this purpose. Our model is based on the very simple expression given in eq. (60), where the trapping time constant is shown to depend mainly on the Fermi level within the channel. From that equation it is evident that a knowledge of the Fermi level dependence on temperature allows us to obtain a good fit of the measured data. In

Appendix C the Fermi energy is calculated down to low temperatures. Let's start to consider what happens at temperatures above about 40 K. Here the classical approximated expression of eq. (A.24) applies. In eq. (60) f_d is very small and we can at first approximate the noise to:

$$\overline{v_{nch}^2} \approx \frac{V_{GS}-V_T}{C_G}\, g_d\, \frac{2e}{c_n}\, \frac{N_d}{N_c^2} \exp\left(2\frac{E_c-E_d^{'}}{K_B T}\right) \frac{1}{1+(\omega\tau_c)^2}, \quad E_d^{'} = E_d + \Delta U_{PF}. \tag{79}$$

Since the statistical fluctuation is proportional to the number of charges, the noise is smaller for small dopant concentrations N_d. This can be seen in the 3D-plot of Figure 20, where the noise for the JFET MX11CD is plotted from below 100 K down to 14 K. The noise at 14 K was close to 400 nV/√Hz due to G-R noise from dopants. This noise in the MX11CD comes from a concentration N_d of a few times 10^{15} atoms/cm^3. Even if eq.(79) were considered valid down to 14 K, the reduction to the nV/√Hz level of this noise would require an unrealistic concentration of about 10^{10} atoms/cm^3.

The approximate eq. (79) is not able to account for the noise at temperatures lower than about 50 K since below this temperature levels the Fermi function f_d can not be considered to be much smaller than one. To fully account for the measured noise the original eq. (60) has been used and in the Fermi function f_d the Fermi energy was that derived in eq. (A.22). The expression (A.22) for the Fermi energy has been obtained assuming that acceptors are generally present inside the channel at a very small concentration. At ordinary temperatures their compensation effect is totally negligible, but when freeze-out occurs they become filled with electrons from dopants and cannot be neglected in the calculations.

The parameters extracted from the spectra of Figure 20, fitted with eq.(63), are listed in Table 12. The very interesting fact can be seen that the Lorentzian frequencies are all found at higher frequencies than the upper measurement range of our instrument, except the one measured at 14 K, which was larger than 30 KHz.

The coefficients A_{LOR} of the G-R noise of Table 12 has then been fitted with a function derived from eq. (60) and eq. (A.22):

$$A_{LOR} = \frac{A_{DOP}}{\sqrt{T}} \frac{f_d^2}{\left[1-f_d+2g_d f_d\right]\left[1-f_d^2\right]}. \tag{80}$$

The fitting parameters that we used were the amplitude A_{DOP}, the effective dopant energy level $E_d^{'} = E_d + \Delta U_{PF}$, the dopant concentration N_d, and the acceptor concentration N_a. In the above equation the term √T comes from c_n, the capture probability rate (see the list of symbols in Table 1). In eq. (60) the term dependent on the gate-to-source voltage and the pinch-off voltage has been considered constant because of the small temperature dependence of V_P in comparison to the other terms. The accuracy of the fitting function with respect to the measured data has been excellent, as can be seen for the continuous curve of Figure 21. The extracted parameters are an amplitude A_{DOP} of about 65000 (nV)^2√K/Hz, a donor concentration of about 0.3×10^{16} atoms/cm^3, a donor energy of $E_d^{'} - E_c = -23\,\text{meV}$, and a concentration of acceptors of 2×10^{13} atoms/cm^3.

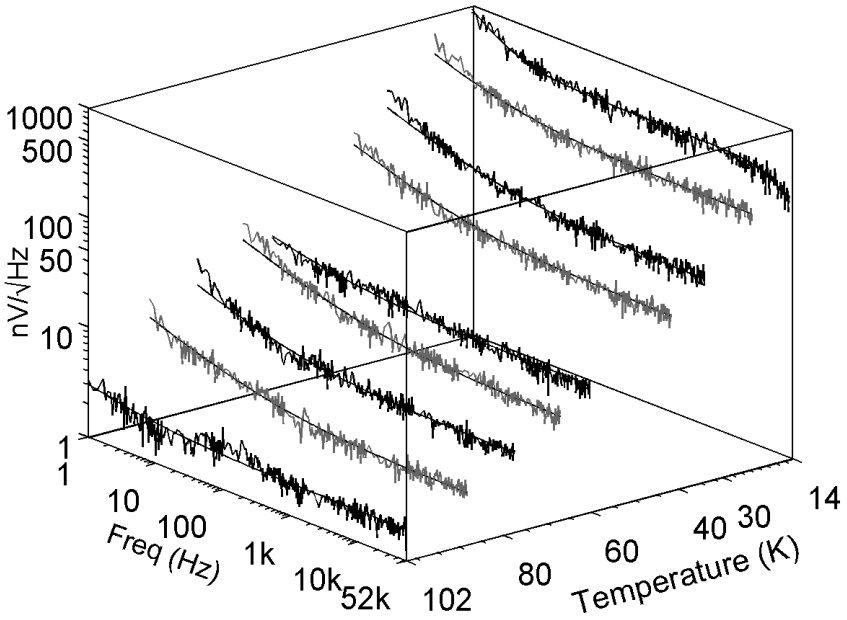

Figure 20: The 3D-plot of the noise spectra measured for the JFET MX11CD in the temperature range 15 K to 100 K. To each noise spectrum the fit is superimposed.

The Poole-Frenkel effect plays an important role in the G-R noise from dopants. In the MX11CD channel the dopants are atoms of phosphorus, which have an ionization energy about 45 meV below the conduction band (measured at room temperature). In the above discussion we estimated ΔU_{PF} to be about -23 meV. The MX11CD is a JFET with a gate length between 1.5 µm and 2 µm. From eq. (78) we expect a barrier lowering between -15 meV and -18 meV, which is quite close to the above extrapolation.

Table 12: Parameters extracted to fit the spectra of **Figure 20**, the series noise of the MX11CD JFET, according to the function of eq.(63).

A_f $[(nV)^2/Hz^{(1-Esp)}]$	Esp	A_{lor} $[(nV)^2/Hz]$	f_{lor} [Hz]	white $[(nV)^2/Hz]$	temperature [^OC]
732560.3	1.220989	155520.3	≥ 33439.16	NA	14.5
161181.7	0.586029	44367.2	>>52k	NA	23
31592.02	0.524504	4785.273	>>52k	NA	33.8
9680.883	0.531088	1494.245	>>52k	NA	41.4
397.5389	0.500001	202.4744	>>52k	NA	60
629.2456	0.520008	74.71638	>>52k	NA	66.7
149.1847	0.567194	27.04342	>>52k	NA	77.1
69.02723	0.53179	8.55076	>>52k	NA	88
5.374359	0.500352	3.671213	>>52k	NA	101.9

In Figure 21 (continuous curve) the fitting of the measured data is very good if a non-negligible acceptor compensation is considered. In the figure it is also plotted the case in which the compensation is assumed totally negligible (dashed curve). At the smaller temperatures the effect of the acceptor atoms is clearly seen.

From eqs. (60) and (80) we derive ($c_n=\sigma v_{th}$):

$$\sigma = \sqrt{\frac{m_n}{3K_B}} \frac{1}{A_{DOP}} \frac{1}{Nd} 4e \frac{V_{GS} - V_T}{C_{GS}} g_d ; \tag{81}$$

The MX11CD was operated at 1 mA of drain current and 1 V of drain to source voltage. The quantity V_{GS}-V_T is estimated to be between 0.5 V and 1 V at 14 K, while the capacitance C_{GS} is about 6 pF. From the above equation we can calculate σ to be between 5×10^{-16} cm^2 and 1.15×10^{-16} cm^2. In Figure 20 we have observed that for the lower temperature investigated the Lorentzian frequency is close to 33 KHz. From eq. (59) and the estimated value for σ and the other parameters of interest, f_{LOR} can be extrapolated to be between 25 KHz and 53 KHz, very close to the measured value. A plot of the Lorentzian frequencies versus temperature is shown in Figure 22, where V_{GS}-V_T is the average between the above-indicated values, or 0.75 V. As can be seen at 14 K, there is a good agreement with the measured value. It can be seen that above about 100 K the Lorentzian frequencies become very large, as expected. Below this temperature the Lorentzian frequencies are under 200 MHz. We are planning to perform an experiment where the frequency range for the measurements for the noise will be sufficient for this temperature interval, in order to prove further the theoretical interpretation we have discussed.

The obtained result proves that Si-JFET transistors cannot be used in low noise applications under 100 K, due to the strong effect of G-R noise from dopant atom sites.

8 CONCLUSIONS

Extensive measurements on the G-R noise of Si-JFET transistors from 14 K up to room temperature has been made on JFETs designed for low noise. It has been shown that around room temperature the main effect comes from deep level traps located in half way between the valence and conduction bands. At the optimum temperature of operation for Si-JFETs, between 100 K and 150 K, the energy of the traps responsible for G-R noise is around 0.1 eV from the band edges. By introducing a mathematical approximation, it was also possible to estimate the concentration of the G-R noise centers. For the very low noise processes that we measured we were able to reach a sensitivity of about 10^{-7} in the ratio between the trapping centers concentration and the dopant concentrations, N_T/N_d.

We were also able to measure the G-R noise coming from dopant atoms themselves inside the channel. To this aim, we re-developed the formulation for the noise and for the Fermi energy. We were then able to show that to obtain a good accuracy of the measured data the effect of the possible presence of a compensated concentration of acceptors cannot be neglected at very low temperatures. We demonstrated that for applications that need low noise at very low temperatures the Si-JFET cannot be used at temperatures below about 100 K.

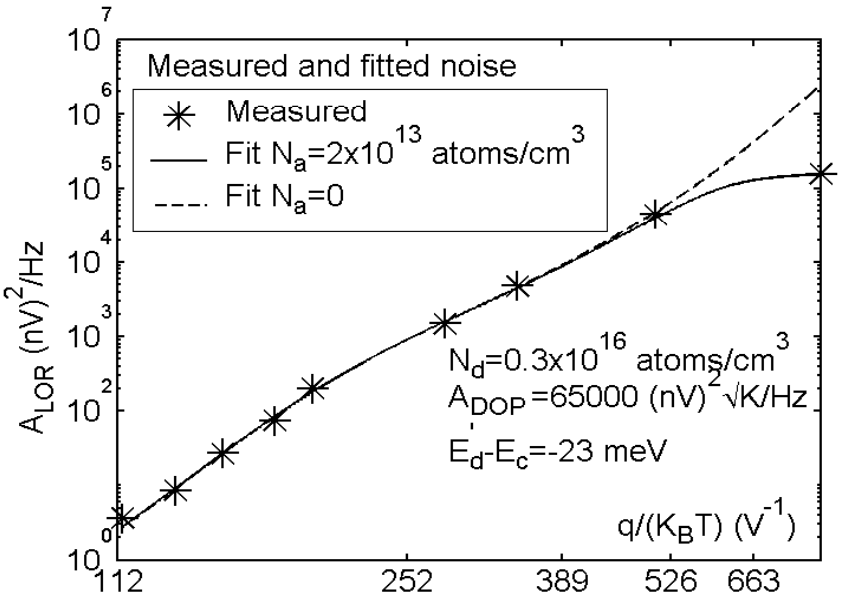

Figure 21: Measured noise amplitude versus 1/T (*) for the MX11CD from 14 K to 100 K. The continuous curve is the fit of the noise according to eq. (80), while the dashed curve does not include the presence of compensated acceptors.

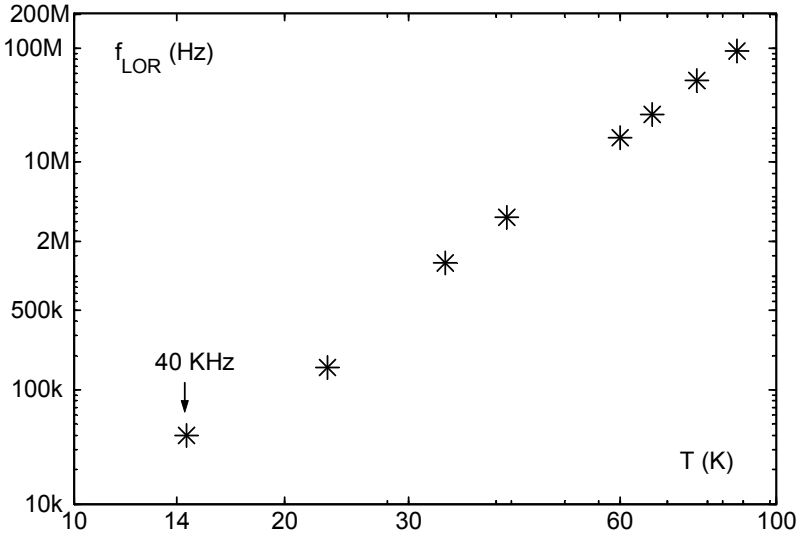

Figure 22: Lorentzian frequencies versus temperature for the G-R noise from dopant atoms, after the parameters extracted from the data in **Figure 21**.

9 APPENDIX A: PROOF OF EQ. (22)

In this appendix we solve eq.(20). This differential equation is easily solved if it is transformed to the form:

$$\frac{dy(t)}{dt} = -k_1 y(t) - k_2 y(t)^2 + h_A \delta(t) . \tag{A.1}$$

To this aim we find a solution n(t) that satisfy: $n(t)=\alpha+y(t)$, with $y(\infty)=0$ and the equilibrium condition α such that $\alpha>0$. This is easily accomplished if α satisfies:

$$\alpha = \frac{-B+\gamma}{2C}, \qquad \text{where} \quad \gamma = \sqrt{B^2 + 4AC} . \tag{A.2}$$

With the above substitution eq.(20) reduces to:

$$\frac{dy(t)}{dt} = -\gamma y(t) - C y(t)^2 + h_A \delta(t) ; \tag{A.3}$$

which is of the form (A.1). It is convenient to seek for a solution of the form: $y(t)=f(t)1(t)$, where f(t) is required to be continuous at t=0. With this condition eq.(A.3) becomes:

$$f(0)\delta(t) + \frac{df(t)}{dt} 1(t) = -\gamma f(t) 1(t) - C f(t)^2 1(t) + h_A \delta(t) ; \tag{A.4}$$

in the above equation use has been made of the properties $d1(t)/dt=\delta(t)$, and $f(t)\delta(t)=f(0)\delta(t)$. Now we put $z(t)=1/f(t)$ and divide both terms of eq.(A.4) by $-f(t)^2$:

$$-z(0)\delta(t) + \frac{dz(t)}{dt} 1(t) = \gamma z(t) 1(t) + C 1(t) - h_A z(0)^2 \delta(t) . \tag{A.5}$$

The terms proportional to 1(t) form a differential eq. that is easily solved when z(t) is of the form:

$$z(t) = \beta_1 \exp(\gamma t) + \beta_2 . \tag{A.6}$$

The function z(t) given above is able to satisfies the whole eq.(A.5) when:

$$z(t) = \left(\frac{1}{h_A} + \frac{C}{\gamma} \right) \exp(\gamma t) - \frac{C}{\gamma} . \tag{A.7}$$

Namely:

$$y(t) = \frac{1(t)}{\left(\frac{1}{h_A} + \frac{C}{\gamma} \right) \exp(\gamma t) - \frac{C}{\gamma}} . \tag{A.8}$$

The condition $n(t)=\alpha+y(t)$ together with the relation given in eq.(A.2) and the above eq.(A.8) is proof of eq.(22) of the text.

10 APPENDIX B: REVIEW OF THE MAIN EQUATIONS GOVERNING JFET OPERATION

The operation of the JFET in the saturation region is easily obtained starting from the Poisson equation given in eq.(42), which is valid for an abrupt junction where p>>n. The

boundary conditions are that at the gate, x=0, the voltage is equal to V_G, while V_S should be the potential at the conducting channel boundary, x=W. In this respect it is assumed that the voltage at the drain, V_D, is close to V_S and the depletion region has a constant width W (see **Figure 4**). The solution of the Poisson eq. is therefore:

$$V(x) = -\frac{1}{2}\frac{e}{\varepsilon} n_{no}(x - W)^2 + V_S + V_{bi} \qquad V(0) = V_G . \tag{A.9}$$

The built-in voltage V_{bi} is added to account for the fact that at zero bias the depletion region has a minimum width, due to the need to balance the diffusion current at the junction. From eq.(A.9):

$$\begin{aligned} W &= \sqrt{\frac{2\varepsilon}{en_{no}}[V_{bi} + V_S - V_G]} \\ &= a\sqrt{\frac{V_{bi} + V_S - V_G}{V_P}} \end{aligned} . \tag{A.10}$$

The channel is completely pinched off when W=a, or, assuming V_S=0 for convenience, when:

$$V_{bi} - V_{GOFF} = V_P = \frac{en_{no}a^2}{2\varepsilon} \quad \text{or} \quad V_{GOFF} = V_{bi} - V_P = V_T . \tag{A.11}$$

The pinch-off voltage, V_P, is an important parameter for low temperature operation. From the equation above we can see that JFET does not work anyway if the threshold voltage, V_T, is greater than zero. This happens at a certain cryogenic temperature since V_{bi} increases and V_P decreases at low temperature. One-way to lower as much as possible the limiting temperature of operation is to choose large value for *a*, the gate thickness[52)].

The current in the channel follows from Ohm's law:

$$\begin{aligned} I_{DS} &= en_{no}Z(a - W)\mu E \\ &\approx en_{no}Z(a - W)\mu\frac{V_{DS}}{L} \end{aligned} . \tag{A.12}$$

Namely:

$$I_{DS} = en_{no}Za\left(1 - \sqrt{\frac{V_{bi} - V_G}{V_P}}\right)\mu\frac{V_{DS}}{L} . \tag{A.13}$$

Finally the last parameter of interest is the transconductance g_m:

$$g_m \doteq \frac{dI_{DS}}{dV_G} = en_{no}Za\,\mu\frac{V_{DS}}{L}\left(\frac{1}{2\sqrt{V_P(V_{bi} - V_G)}}\right) . \tag{A.14}$$

The last two equations can be given a more compact form that is valid whenever the channel current I_{DS} is much smaller than I_{DSS}, the current expected at V_{GS}=0 V. For this case eq.(A.13) can be expanded around $V_G=V_T$ giving:

$$I_{DS} = en_{no} Za\,\mu \frac{V_{DS}}{L}\frac{1}{2}\frac{V_G - V_T}{V_P}. \tag{A.15}$$

Consequently, the transconductance, g_m, can be expressed as:

$$g_m = en_{no} Za\,\mu \frac{V_{DS}}{L}\frac{1}{2}\frac{1}{V_P}; \tag{A.16}$$

or:

$$\frac{I_D}{g_m} = V_G - V_T. \tag{A.17}$$

11 APPENDIX C: THE FERMI LEVEL IN A SEMICONDUCTOR

In an n-type semiconductor there is always a certain degree of compensation due to the presence of acceptors. The effects of these dopants can be very small and totally negligible at ordinary temperatures. At cryogenic temperatures this is not the case and electrons tend to fill, or freeze out, at both the n-type and the p-type dopant atoms. So the actual concentration of electrons in the conduction band satisfies the condition $n+N_{a-}(T)=(N_d-n_d)$, where $N_{a-}(T)$ represents the concentration of acceptor centers that are not filled, $N_{a-}(300)\approx 0$ while $N_{a-}(0)\approx N_a$. This compensation effect is negligible at ordinary temperatures, but it is effective under about 40 K[60]. This has been taken into account in deriving the fitting of the noise measurements at the lower temperatures.

Eq.(39) for the case of dopants must be written:

$$\frac{n_d}{n + N_{a-}(T)} = \frac{n_d}{n'} = \frac{g_d f_d}{1 - f_d}; \tag{A.18}$$

while f_d from eq.(38) is:

$$f_d = \frac{1}{1 + \exp[(E_d - E_F)/K_B T]}. \tag{A.19}$$

By considering that $N_d=n_d+n'$ and that $n = N_C \exp\left(\frac{E_F - Ec}{K_B T}\right)$ we can write:

$$\frac{1}{1+\exp[(E_d - E_F)/K_B T]} = \frac{1 - \frac{N_{a-}(T)}{N_d} - \frac{N_C}{N_d}\exp\left(\frac{E_d - E_C}{K_B T}\right)\exp\left(\frac{E_F - E_d}{K_B T}\right)}{1 + (g_d - 1)\left[\frac{N_{a-}(T)}{N_d} + \frac{N_C}{N_d}\exp\left(\frac{E_d - E_C}{K_B T}\right)\exp\left(\frac{E_F - E_d}{K_B T}\right)\right]} \tag{A.20}$$

Namely:

$$\frac{1}{1+x}=\frac{1-z-\frac{y}{x}}{1+(g_d-1)\left[z+\frac{y}{x}\right]},\quad x=\exp\left(\frac{E_d-E_F}{K_BT}\right),\quad y=\frac{N_C}{N_d}\exp\left(\frac{E_d-E_C}{K_BT}\right),\quad z=\frac{N_{a-}(T)}{N_d} \qquad (A.21)$$

Eq.(A.21) is a second order equation in the variable x. Considering that we are interested in a solution with x>0, after a few mathematical manipulations the expression for the Fermi level becomes:

$$E_F=E_c-K_BT\ln\left\{\frac{N_c}{N_d}\frac{1+gz/y}{2(1-z)}\left[1+\left(1+\frac{4gy(1-z)}{(y+gz)^2}\right)^{1/2}\right]\right\}. \qquad (A.22)$$

In eq. (A.22) there is a dependence on temperature of z that complicates the final expression. To simplify it is convenient to consider $N_{a-}(T)=N_a$ for temperatures lower than about 40 K and $N_{a-}(T)=0$ above that range. For T>40 K eq. (A.22) simplifies to:

$$E_F=E_c-K_BT\ln\left\{\frac{N_c}{N_d}\frac{1}{2}\left[1+\left(1+\frac{4g_d}{y}\right)^{1/2}\right]\right\}. \qquad (A.23)$$

In addition, in the case that N_d is sufficiently small ($4g_d/y\approx 0$) from above we can obtain the classical expression:

$$E_F=E_c-K_BT\ln\left(\frac{N_c}{N_d}\right). \qquad (A.24)$$

12 ACKNOWLEDGEMENTS

We thank Maurizio Perego for accurate layout of the boards used for noise characterization. We thank the staff of the Central Library of the Università della Bicocca for helping us in finding some of the papers and books text that we have used as references.

13 REFERENCES

(1) R.C.Jones, The general theory of bolometer performance, *Jour. of the Opti. Soci. of America*, V.43, p.1-14, 1953.

(2) A.Alessandrello, J.W.Beeman, C.Brofferio, O.Cremonesi, E.Fiorini, A.Giuliani, E.E.Haller, A.Monfardini, A.Nucciotti, M.Pavan, G.Pessina, E.Previtali, L.Zanotti, High energy resolution bolometers for nuclear and X-ray spectroscopy, *Physical Review Letters,* V.82, p.513-515, 1999.

(3) A.Alessandrello, C.Brofferio, C.Cattadori, R.Cavallini, O.Cremonesi, L.Ferrario, A.Giuliani, B.Margesin, A.Nucciotti, M.Pavan, G.Pessina, G.Pignatel, E.Previtali, M.Sisti, Fabrication and low temperature characterization of Si-implanted thermistors, *J. Phys. D: Appl. Phys.*, V.32, p.3099-3110, 1999.

(4) K.K.Wang, A.van der Ziel, E.R.Chenette, Neutron-induced noise in JFET, *IEEE Trans. on Elec Devices,* V.ED-22, p.591-593, 1975.

(5) P.F.Manfredi, L.Ratti, V.Re, V.Speziali, Noise degradation induced by γ rays on p- and n-channel JFET, *IEEE Tr. on Nucl. Sci.,* V.46, p.1294-1299, 1999.

(6) F.N.Hooge, 1/f noise sources, *IEEE Trans. on Elec Devices,* V.ED-41, p.1926-1935.

(7) S.Christensson, I.Lundstrom, C.Svensson, Low frequency noise in MOS transistors-I, *Solid-State Elec,* V.11, p.797-812, 1968.

(8) S.Christensson, I.Lundstrom, Low frequency noise in MOS transistors-II experiments, *Solid-State Elec,* V.11, p.813-820, 1968.

(9) E.Simoen, C.Claeys, The low-frequency noise behavior of Silicon-on-insulator technologies, *Solid-State Elec,* V.39, p.949-960, 1996.

(10) E.Simoen, C.Claeys, On the flicker noise in sub-micron silicon MOSFETs, *Solid-State Elec,* V.43, p.865-882, 1999.

(11) N.Lukyanchikova, N.Garbar, M.Petrichuk, E.Simoen, C.Claeys, Flicker noise in deep sub-micron nMOS transistors, *Solid-State Elec,* V.44, p.1239-1245, 2000.

(12) W.Shockley, W.T.Read Jr, Statistics of the recombination of Holes and Electrons, *Phys. Review,* V.87, p.835-842, 1952.

(13) G.Bemski, Recombination in semiconductors, *Proc. of the IRE,* V.46, p.990-1004, 1958.

(14) W.Shockley, Electrons, Holes and Traps, *Proc. of the IRE,* V.46, p.973-990, 1958.

(15) K.Kandiah, M.O.Deighton, F.B.Whiting, A physical model for random telegraph signal currents in semiconductor devices, *J. Appl. Phys.,* V.66, p.937-948, 1989.

(16) K.Kandiah, Random telegraph signal currents and low-frequency noise in JFET, *IEEE Trans. on Elec Devices,* V.ED-41, p.2006-2015, 1994.

(17) M.J.Uren D.J.Day, M.J.Kirton, 1/f and random telegraph noise in silicon metal-oxide-semiconductor FET, *Appl. Phys. Lett.,* V.47, p.1195-1197, 1985.

(18] E. Gatti, A. Longoni, R. Sacco, Trapping noise in semiconductor devices: a method for determining the noise spectrum as a function of the trap position, *J. Of Appl. Physics,* V.78, p.6283-6297, 1995.

(19) F.N.Hooge, L.Ren, On the variances of generation-recombination noise in a three-level system, *Physica*, V. B193, p.31-38, 1994.

(20) S.Machlup, Noise in semiconductors: spectrum of a two-parameter random signal, *J. Of Appl. Physics,* V.25, p.341-343, 1954.

(21) A.D.Van Rheenen, G.Bosman, C.M. van Vliet, Decomposition of generation-recombination noise spectra in separate Lorentzians, *Solid-State Elec.,*V.28, p.457-463, 1985.

(22) C.T.Sah, Theory of low-frequency Generation noise in JFET, *Proc. of IRE,* V.52, p.795-814, 1964.

(23) P.O.Lauritzen, Low-frequency generation noise in JFET transistors, *Solid State Elec.,* V.8, p.41-58, 1965.

(24) L.D.Yau, C.T.Sah, Theory and experiments of low-frequency Generation-Recombination noise in MOS transistors, *IEEE Trans. on Elec Devices,* V.ED-16, p.170-177, 1969.

(25) K.K.Hung, P.K.KO, C.Hu, Y.C.Cheng, A unified model for the flicker noise in metal-oxide-semiconductor Field-Effect transistors, *IEEE Tran. On Elc. Devices,* V.37, p.654-665, 1990.

(26) R.A.Smith, Semiconductors, II Edition, Cambridge University Press, 1978, p. 282-283.

(27) R.E.Burgess, Fluctuations in the number of charge carriers in a semiconductor, *Physica XX*, V.11, p.1007-1010, 1954.

(28) R.E.Burgess, Fluctuations of the numbers of electrons and holes in a semiconductor, *Proc. of the Physical Society*, V.B68, p.661-671, 1955.

(29) M.Lax, Fluctuations from non-equilibrium steady state, Reviews of Modern Physics, V.32, p.25-64, 1960.

(30) R.E.Burgess, The statistics of charge carrier fluctuations in semiconductors, *Proc. of the Physical Society*, V.B69, p.1020-1027, 1956.

(31) F.N.Hooge, L.Ren, On generation-recombination noise, *Physica*, V. B191, p.220-226.

(32) A.Van der Ziel, Carrier density fluctuation noise in FET, *Proc. of IEEE*, V.51, p1670-1671, 1963.

(33) D.C.Murray, A.G.R.Evans, J.C.Carter, Shallow defects responsible for GR noise in MOSFET's, *IEEE Trans. on Elec Devices,* V.ED-38, p.407-416, 1991.

(34) F.Scholz, J.M.Hwang, D.K.Schroder, Low frequency noise and DLTS as semiconductor device characterization tools, *Solid-State Elec.,* V.31, p.205-217, 1988.

(35) SKUDOTECH® is a Registered trademark by SELITE, Via Aurelio Saffi 29, 20123 Milano, IT.

(36) A.Alessandrello, C.Brofferio, O.Cremonesi, A.Giuliani, A.Monfardini, A.Nucciotti, M.Pavan, G.Pessina and E.Previtali, A Front-End for an Array of μ-Bolometers for the Study of the Neutrino Mass, *IEEE on Nucl. Scie.,* V.47, p.1851-1856, 2000.

(37) E.A.Hendriks, R.J.J.Zijlstra, Field-induced generation-recombination noise in (100) n-channel Si-Mosfet's at T=4.2 K, *Physica,* V.147B, p.291-296, 1987.

(38) S.Kugler, Generation-recombination noise in the saturation regime of MODFET structures, *IEEE Trans. on Elec Devices,* V.ED-35, p.623-628, 1988.

(39) V.Grassi, C.F.Colombo, D.V.Camin, Low frequency noise versus temperature spectroscopy of recently designed Ge JFETs, *IEEE Tr. on Nucl. Scie*, V.48, p.2899-2005, 2001.

(40) K.Kandiah, F.B.Whiting, Limits of resolution of charge sensitive detectors systems, *Nucl. Instr. And Meth. A,* V.A326, p.49-62, 1993.

(41) K.Kandiah, F.B.Whiting, Nonideal behavior of buried channel CCDs caused by oxide and bulk silicon traps, *Nucl. Instr. And Meth. A,* V.A305, p.600-607, 1991.

(42) K.Kandiah, F.B.Whiting, Low frequency noise in JFET transistors, *Solid-State Elec.,* V.21, p.1079-1088, 1978.

(43) A.D.van Rheenen, G.Bosman, R.J.J.Zulstra, Low frequency measurements as a tool to analyze deep-level impurities in semiconductor devices, *Solid-State Elec.,* V.30, p.259-265, 1987.

(44) F.J.Scholz, J.W.Roach, Low frequency noise as a tool for characterization of near-band impurities in silicon, *Solid-State Elec.,* V.35, p.447-452, 1992.

(45) J.W.Haslett, E.J.M.Kendall, Temperature dependence of low-frequency excess noise in JFET, *IEEE Trans. on Elec Devices,* V.ED-19, p.943-, 1972.

(46) W.H. Press, B.P. Flannery, S.A. Teukoslsky, W.T. Vetterling, Numerical Recipes in C++, Cambridge University Press, 2002, p.704-711.

(47) D.V.Camin, C.F.Colombo, V.Grassi, Low frequency noise versus temperature spectroscopy of Ge JFETs, Si JFETs and Si MOSFETs, Journal de Physique IV (Proceedings), V. 12, 2002, p. Pr3-37.

(48) A. Fascilla, G. Pessina, A very simple method to measure the input capacitance and the input current of transistors, *Nucl. Instr. And Meth. A,* V. A469, p.116-126, 2001.

(49) M.W.Lund, K.W.Decker, R.T.Perkins, J.D.Phillips, Low noise JFETs for room temperature x-ray detectors, *Nucl. Instr. And Meth*, V.A380, p.318-322, 1996.

(50) A.Alessandrello, C.Brofferio, O.Cremonesi, A.Fascilla, A.Giuliani, Mark W. Lund, A.Nucciotti, M.Pavan, G.Pessina, E.Previtali, Low noise silicon JFETs working at low temperatures for bolometric detector readout, 'WOLTE 4, 4st European Workshop on Low Temperature Electronics', p.137-141, 2000.

(51) F.J.Morin, J.P.Maita, Electrical properties of Silicon containing Arsenic and Boron, *Physical Review*, V.96, p.28-35, 1954.

(52) J.W.Haslett, E.J.Mkendall, F.J.Scholz, design considerations for improving low-temperature noise performance of Silicon JFET, *Solid-State Elec.,* V.18, p.199-207, 1975.

(53) C.Jacoboni, C.Canali, G.Ottavaini, A.Alberigi Quaranta, A review of some charge transport properties of silicon, *Solid-State Elec,* V.20, p.77-89, 1977.

(54) A.Van Der Ziel, Fisica dei dispositivi elettronici a stato solido, III Edizione, Liguori Editore (translation from Solid State Physical Electronics, Prentice Hall, Inc.), 1979, p.554-556.

(55) B.Lengeler, Semiconductor devices suitable for use in cryogenic environments, *Cryogenics*, Vol. 40, p. 439-447, 1974.

(56) K.Takagi, K.Matsumoto, Noise in silicon and JFET's at high electric fields, *Solid-State Elec.,* V.20, p.1-3, 1977.

(57) F.M.Klassen, J.R.Robinson, Anomalous noise behavior of JFET transistors at low temperatures, *IEEE Trans. on Elec Devices,* V.ED-17, p.852-857, 1970.

(58) R.Jayaraman, C.G.Sodini, A 1/f noise technique to extract the oxide trap density near the conduction band edge of silicon, *IEEE Trans. on Elec Devices,* V.ED-36, p.1773-1782, 1989.

(59) B.Dierickx, E.Simoen, S.Cos, J.Vermeiren, C.Claeys, G.J.Declerck, Anomalus kink-related excess noise in MOSFET'' at 4.2 K, *IEEE Trans. on Elec Devices,* V.ED-38, p.907-912, 1991.

(60) M.Shur, Physics of semiconductor devices, Prentice Hall, p. 54-66,1990.